DETERMINATION OF VITAMIN D BY SENSOR TECHNOLOGIES BASED ON MOLECULAR IMPRINTED POLYMERS

A Thesis Submitted to
the Graduate School of Engineering and Sciences of
İzmir Institute of Technology
in Partial Fullfillment of the Requirements for the Degree of

DOCTOR OF PHILOSOPHY

in Materials Science and Engineering

by
Yekta Arya ÖLÇER ALTINSOY

July 2022
İZMİR

ACKNOWLEDGEMENT

I would like to acknowledge the help of many people during my study. Firstly, I would like to express my special thanks to my advisor Prof. Dr. Ahmet E. EROĞLU for his guidance, care and freedom that he provided me throughout the study. One simply could not wish for a better or friendlier supervisor. I am also grateful to my co-advisor Prof. Dr. Mustafa M. DEMİR for valuable discussions, encouragement and support during my thesis. I would like to thank to other members of the thesis committee, Assoc. Prof. Dr. Ezel BOYACI, Assoc. Prof. Dr. Yaşar AKDOĞAN, Assoc. Prof. Dr. Aziz GENÇ and Assoc. Prof. Dr. Aylin ZİYLAN for their valuable comments and suggestions. Also I would like to thank you to Dr. Asuman ÜNAL for her encouragement and support.

I would like to extend my sincere thanks to the research scientists at the Centre for Materials Research (IZTECH) for their help on facilities SEM. I would like to thank to TÜBİTAK for financial support.

Thanks to my colleagues and Analytical Chemistry Research Group lab mates for their support and positive input. I deeply thank to my sister Merve DEMİRKURT AKBAL firstly for her true friendship and then her help during not only my PhD studies also my MSc and undergraduate education. I would also like to thank my other sister Hazal TOSUN for her true friendship, advices and encouragements.

My deepest gratitude goes to my lovely spiritual sister Tuğba IŞIK for her encouragement and never ending friendship starting from the high school. I am so lucky to have such best friend.

I wish to thank all of my lovely family. My mom Özlem ÖLÇER and my father Mehmet ÖLÇER have always supported me with endless love and patience throughout my whole education life. They always made me feel their love and support in all circumstances. I would like to express my special thanks to my husband Sefa Can ALTINSOY that he supported my PhD studies with love and patience. Especially during the writing part of this thesis I am so thankful for his unending patience. Also, Dobi, Çapkın and Barney (my little dogs) have shown their supports and encouragements during my education life. I am so lucky to have such a good and big family and indebted to them for their unending love, so I dedicate this thesis to my whole family.

ABSTRACT

DETERMINATION OF VITAMIN D BY SENSOR TECHNOLOGIES BASED ON MOLECULAR IMPRINTED POLYMERS

Vitamin D is an essential nutrient in the body; it plays important roles in human health. Both its lack and excess can have health risks. As a consequence, there is a great demand for development of simple and precise detection methods for vitamin D derivatives in different samples. Molecular imprinting polymers (MIPs) are artificial receptors that can recognize target molecules in solution. In this study, two different polymerization techniques were used to obtain MIP/NIP sorbents/films for the detection of vitamin D3. Firstly, molecular imprinted solid phase extraction (MISPE) method was proposed prior to HPLC-DAD analysis. Optimized parameters were as follows; sorbent amount of 5.0 mg for 5.0 mL of 1.0 mg/L vitamin D3 in 90:10 (v/v) ratio of H_2O:MeOH solution, 5 hours sorption time and MeOH:HOAc ratio of 90:10 (v/v) as desorption solution. The accuracy of the method was verified with spike recovery test for PBS:MeOH in a ratio of 90:10 (v/v) and overall recovery was found as 85.1 (±4.3, n=3).

In latter case, a quartz crystal microbalance (QCM) method was proposed for determination of vitamin D3. Electrochemical polymerization of poly(4-vinylpyridine) MIP/NIP films were achieved on gold working electrode by cyclic voltammetry (CV). Mass-transfer ability of the polymer films were analyzed by electrochemical impedance spectroscopy (EIS). The electrochemical QCM (eQCM) was used to develop thin polymer films on quartz crystals and vitamin D3 determination was achieved by QCM. In a preliminary test, as small a concentration as 0.0100 mg/L vitamin D was detected with the QCM method.

ÖZET

MOLEKÜLER BASKILANMIŞ POLİMERLER TEMELLİ SENSÖR TEKNOLOJİLERİ İLE D VİTAMİNİ TAYİNİ

D vitamini vücut için önemli bir besindir ve insan sağlığında önemli rol oynar. Eksikliği de fazlalığı da sağlık açısından risk oluşturabilir. Bu sebeple, çeşitli numune matrikslerinde D vitamini türevlerinin tayini için basit ve kesin yöntemlerin geliştirilmesi büyük önem taşımaktadır. Moleküler baskılanmış polimerler, çözeltideki hedef molekülleri tanıyabilen yapay reseptörlerdir. Bu çalışmada, D3 vitamini tayini için MIP/NIP sorbentleri/filmleri elde etmek amacıyla iki farklı polimerizasyon tekniği kullanılmıştır. İlk olarak, HPLC-DAD analizinden önce moleküler baskılanmış katı faz ekstraksiyonu (MISPE) yöntemi önerilmiştir. Optimize edilmiş parametreler; 90:10 (v/v) H_2O:MeOH numune matriksi, 5.0 mL 1.0 mg/L D3 vitamini için 5.0 mg sorbent miktarı, 5 saat sorpsiyon süresi ve 90:10 (v/v) MeOH:HOAc desorpsiyon çözeltisidir. Yöntemin doğruluğu, 90:10 (v/v) PBS:MeOH için geri kazanım testi ile doğrulanmıştır ve toplam geri kazanım 85.1 (±4.3, n=3) olarak bulunmuştur.

İkinci kısımda, D3 vitamini tayini için kuvars kristal mikrobalans (QCM) yöntemi önerilmiştir. Poli(4-vinilpiridin) MIP/NIP filmlerinin elektrokimyasal polimerizasyonu, döngüsel voltametri (CV) ile altın çalışma elektrotu üzerinde gerçekleştirilmiştir. Polimer filmlerin kütle transfer kabiliyeti elektrokimyasal empedans spektroskopi (EIS) ile analiz edilmiştir. Elektrokimyasal QCM (eQCM), kuvars kristalleri üzerinde ince polimer film oluşturmak için kullanılmıştır ve D3 vitamini QCM ile tayin edilmiştir. Bu yöntem ile 0.0100 mg/L D3 vitamini miktarı belirlenebilmiştir.

TABLE OF CONTENTS

LIST OF FIGURES

Figure **Page**

Figure **Page**

LIST OF TABLES

Table **Page**

CHAPTER 1

INTRODUCTION

1.1. Vitamin D and Its Derivatives

Vitamin D is a hormone precursor. It has two different forms; vitamin D2 and D3. Vitamin D2 and its provitamin form (ergosterol) are found in plants, fungi and some invertebrates. Vitamin D3 is synthesized from the skin precursor 7-dehydrocholesterol with the effect of UVB radiation. Figure 1.1 shows the structures of cholecalciferol (vitamin D3), ergocalciferol (vitamin D2), 7-dehydrocholesterol (provitamin D3), and ergosterol (provitamin D2). 7-dehydrocholesterol and ergosterol have steroidal structures that are composed of four fused rings with three six membered cyclohexane ring and one five member cyclopentane ring. Vitamin D3 and Vitamin D2 have secosteroid structure that is a steroid molecule with one ring open. The main structure difference of vitamin D3 and vitamin D2 is the double bond and a methyl group at side chain. This structure difference also occurs in their provitamins.

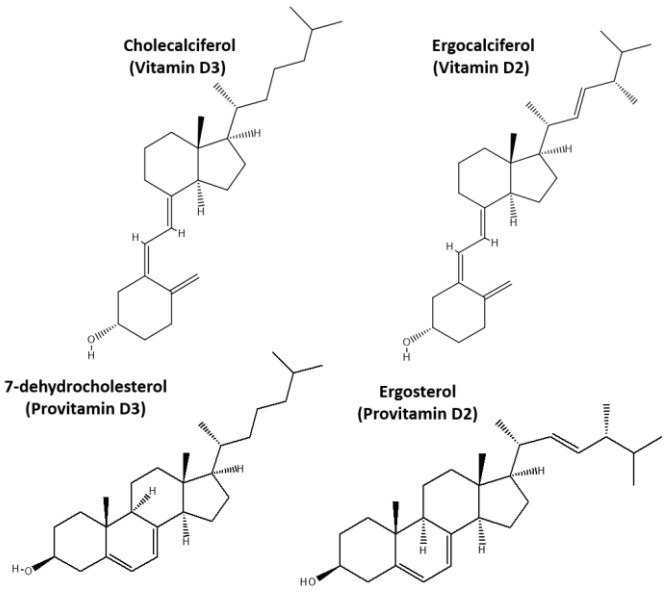

Figure 1.1. The structures of cholecalciferol (vitamin D3), ergocalciferol (vitamin D2), 7-dehydrocholesterol (provitamin D3), and ergosterol (provitamin D2).

Vitamins D2 and D3 are required to undergo a variety of metabolic processes to be converted to the active forms in the body (Kasalová et al., 2015). The metabolism of vitamins D2 and D3 is shown in Figure 1.2. When vitamin D3 is concerned, it is seen that 7-dehydroxycholesterol (provitamin D3) in the skin is converted to previtamin D3 by exposure to UVB radiation from sunlight. With thermal isomerization, previtamin D3 is converted to the familiar form of vitamin D3. Vitamins D2 and D3 taken with dietary supplements follow the same path in the body. Even though there are two separate forms, vitamins D2 and D3 have the same function in body. These vitamins are converted to hydroxy forms (25-hydroxyvitamin D3 (25(OH)D3) and 25-hydroxyvitamin D2 (25(OH)D2) by the enzyme 25-hydroxylase in the liver. Vitamin D test is performed on these hydroxy forms. The total amount of 25(OH)D3 and 25(OH)D2 in the blood provides information about vitamin D deficiency/excess/sufficiency. Dihydroxy forms are then obtained in the kidneys with the enzyme 1α-hydroxylase. Both the hydroxy and dihydroxy forms are active forms that function in the body (Jäpelt and Jakobsen, 2013). In order to prevent vitamin D poisoning, the excess vitamin can be simultaneously converted into photolysis inactive products (lumisterol and tachisterol) and biological inactive products (24-25 dihydroxy vitamin D and 1,24,25 trihydroxy vitamin D).

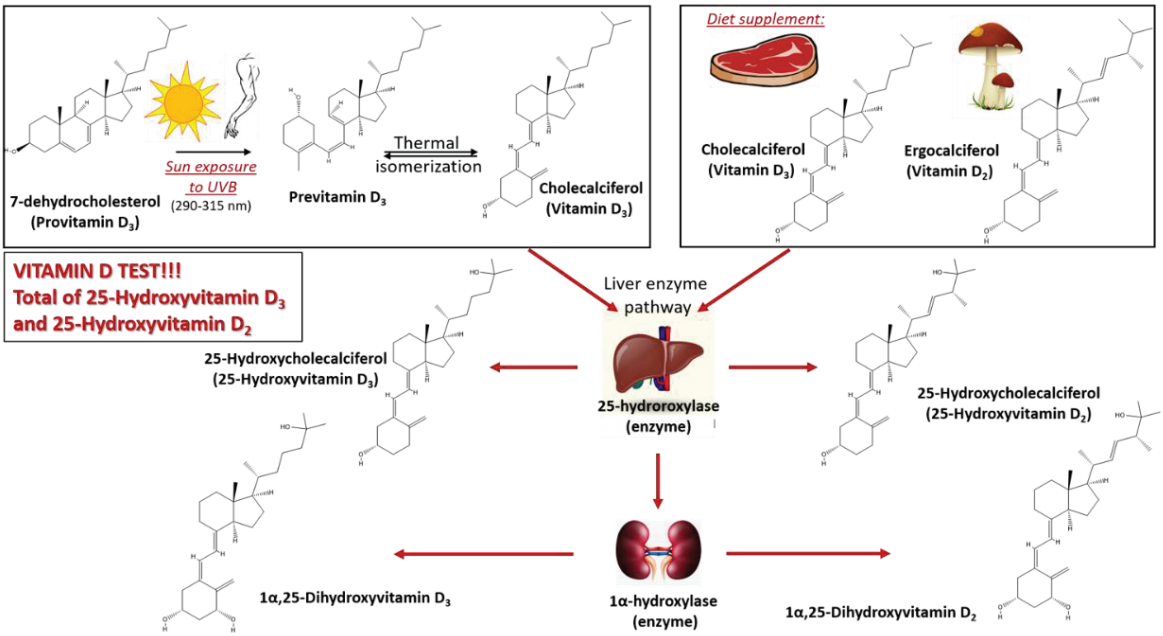

Figure 1.2. The metabolism of vitamin D2 and D3 in body.

Daily vitamin D requirement varies according to the age of the individual. The Institute of Medicine (IOM) determines the daily dose as 15 µg for adults, 10 µg for children and 20 µg for people over 70 years of age (Bendik et al., 2014). The maximum daily limit is 100 µg. According to Table 1.1, 12.5 nmol/L and below shows severe deficiency, 12.5-25 nmol/L deficiency, 25-50 nmol/L insufficiency and 50 nmol/L saturation (repletion). The above-mentioned study reported the factors affecting vitamin D synthesis as the amount of UVB reaching the skin, age, skin color, air pollution in large cities (Mousavi et al., 2019), inadequate outdoor activity, inactivity of older people, and differences in cultural dressing styles. These factors can lead to vitamin D deficiency or poisoning in an individual. Vitamin D deficiency can cause diseases such as rickets, prostate cancer, breast cancer, diabetes, depression (Altinbas et al., 2019). Intoxication can cause hypercalcemia, hyperphosphatemia and hypercalciuria. For this reason, it is very important that the amount of vitamin D in the blood is balanced and precisely determined. Roth et al. (2018) reported that 51% of the population in Turkey has vitamin D deficiency.

Table 1.1. Conditions where vitamin D amounts correspond to blood tests (left) and daily vitamin D requirement (right).

▪ Severe deficiency → < 12.5 nmol/L ▪ Deficiency → 12.5-25 nmol/L ▪ Insufficiency → 25-50 nmol/L ▪ Repletion → 50 nmol/L	▪ Dietary allowance → 15 µg/day ▪ Children → 10 µg/day ▪ > 70 (age) → 20 µg/day ▪ Upper intake → 100 µg/day

1.1.1. Determination of Vitamin D

In literature, there are studies using commercial SPE columns for the determination of 25(OH)D3 and 25(OH)D2 (Rezayi et al., 2018). The most common of these are Sep-Pak silica and C-18 columns. In a the study by Bodnar et al., 2007 Sep-Pak C18 and silica cartridges were used and 25(OH)D3 in the serum of pregnant women in the northern US and in the cord blood of newborns was determined by HPLC. In another study, the total amount of serum 25(OH)D was determined by competitive protein binding assay (CPBA) and HPLC (Rapuri et al., 2004). Sep-Pak C-18/OH and silica cartridges were used for the extraction and purification of serum samples. In the study of

Knox et al. (2009) 25(OH)D3 was measured by SPE method using Orochem C8 commercial cartridge. Hexadeuterate 25(OH)D3 was used as internal standard and the method was applied to serum and plasma. Protein was then precipitated using methanol and purified samples containing 25(OH)D3 and 25(OH)D2 were analyzed by LC-MS/MS.

There are very few studies in the literature on the determination of vitamin D with imprinted polymers. In one study, cholesterol was used as the template and the synthesized MIP was applied to determination of cholesterol, ergesterol, dehydroergesterol and vitamin D3 (Wybranska et al., 2008). In a study by Hashim et al. (2016), ergesterol, which is the precursor of vitamin D2, was used as the template. First, the ergosteryl-3-O-methacrylate template-monomer compound was synthesized, then EGDMA was used as cross-linker and MIP synthesis was performed.

1.1.2. Stability of Vitamin D

Vitamin D is fat soluble. The solubility of these compounds are high in non-aqueous media like ethanol, methanol, and isopropyl alcohol. However, they have restricted solubility in aqueous media. Also, they are very sensitive to oxygen, light and presence of metal ions.

Temova Rakuša et al. (2021) investigated the influence of media, temperature, light, oxygen, pH, concentration, and metal ions on Vitamin D3 stability. They used HPLC-UV for analysis and followed the concentration decrease for each influence. They found that the vitamin D3 is stable in non-aqueous solutions. For aqueous solutions, it is more stable in high purity water (Milli-Q), tap water (TW) and distilled water (DW), respectively. The authors used temperatures of 4, 25, and 40 °C in aqueous solutions and reported that as the temperature increases the stability decreases. Direct exposure to the light and oxygen also decreases the stability. For the pH of the solution, it was said that vitamin D3 is stable for pHs greater than 5. The effect of Vitamin D3 concentration was also investigated for 10 mg/L, 25 mg/L, 100 mg/L, 500 mg/L in water-methanol (90:10 v/v) mixture and found that the higher the concentration the higher the stability in aqueous media. However, in real samples they found that as the concentration increases, stability decreases. Also, the presence of metal ions (Fe^{2+}, Cu^{+} and Cu^{2+}) also decreases the

stability, behaving as catalyst for oxidation of vitamin D3. They concluded that vitamin D3 degradation is still unclear and complex.

1.2. Sample Preparation Methods for the Chromatographic Techniques

A pretreatment/sample manipulation step is usually required before the chromatographic determination of many analytes due to the presence of the undesired components of chemical matrix of difficult samples. Otherwise, the determination step might be inaccurate because of interference effects. Sample pretreatment step is also accompanied with a preconcentration step where the analyte concentration is low to be detected. Solid phase extraction, solid phase micro-extraction, liquid-liquid extraction (solvent extraction), electrodeposition, ion exchange and membrane filtration are among the generally used methods for separation and pre-concentration of selected analytes from samples. In this thesis solid phase extraction method will be used for the selective determination of vitamin D3.

1.2.1. Solid Phase Extraction (SPE)

Solid phase extraction (SPE) is a powerful method for the enrichment and purifying analytes from samples. The main advantages of this method over other methods are fast and easy manipulation, less solvent consumption and high pre-concentration factors. Figure 1.3 shows four basic steps of SPE. In conditioning step, sorbent is wetted and rinsed by the eluting solvent. Secondly, loading is achieved by passing a liquid sample through a short column of a solid sorbent for the sorption of desired compounds. During rinsing step, removal of unwanted compounds is achieved by rinsing with a suitable solvent. Last step is elution. A pre-determined solvent is used for the elution of the analytes. The reproducibility of the method is also determined by this step.

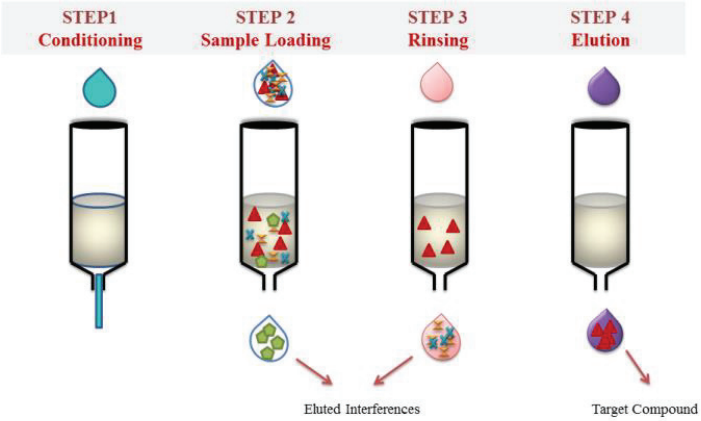

Figure 1.3. Basic steps of solid phase extraction.

Column and batch type solid phase extractions can be used for enrichment and purifying. In the column type SPE (Figure 1.4 (a)), firstly the column is loaded with sample. Analyte is sorbed by the solid sorbent. Recovery is achieved with a little amount of eluent. The concentration of the analyte in the eluate gives the percentage of elution. In the batch type (Figure 1.4 (b)), the solid sorbent is directly put into the sample solution and shaken. After filtration, the analytes are desorbed with a solvent. For both types total recovery is calculated as in Equation 1.1.

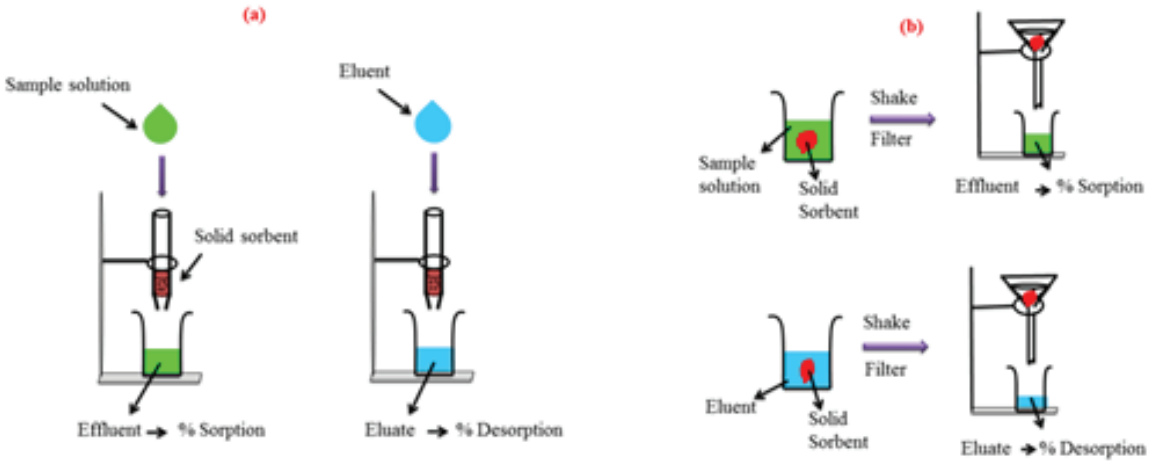

Figure 1.4. Solid Phase Extraction Types (a) Column type SPE, (b) Batch type SPE.

$$\text{Total Recovery} = \frac{[\text{analyte}]\text{eluate}}{[\text{analyte}]\text{sample}} \times 100 \qquad \text{Equation 1}$$

For both SPE processes, to have a successive enrichment/purifying, the key is to choose the most proper sorbent that have the necessary functionality to interact with the analyte. The types of sorbent are generally classified as hyper-crosslinked sorbents, hydrophilic sorbents, mixed mode polymeric sorbents and molecular imprinted polymers. In this thesis we will focus on molecular imprinted polymers.

1.2.1.1. Molecular Imprinted Polymers

The recognition ability of receptors to only one type of substance among other species make them very attractive to scientists. Receptors can easily distinguish their own partner molecule and make stable complexes. This naturally occurring receptors are also found in our body. They are responsive for many processes which are essential for existence. Nowadays scientists are interested in creating new molecules by imitating these natural receptors. These artificial receptors do not only deal with proteins like the natural ones in body. Specific or selective receptors may be created for different compounds. Stability, flexibility and activity in different conditions can be controlled. With a proper chemical design, materials that has the sites completely suited to an analyte can be created. This process can be named as 'molecular recognition', which is the key idea behind 'molecular imprinted polymers'.

Relatively economic synthesis procedure is one of the most imported advantages of MIPs. For example, the usage of the receptor is a common method for the treatment of wastewater. However, its cost is quite high. MIP can be put into use as an inexpensive method. Also, it is very easy to prepare the MIP in a short time. High stability and activity during a wide range of conditions in addition to robustness are the other advantages. Selective and strong binding sites against analytes make it very proper for the usage in an SPE method.

Synthesis of MIP is achieved by the polymerization of monomer(s) and crosslinking agent around the template molecule. For the MIP synthesis, it can be thought that generally the cross-linker is polymerized. Crosslinking agent supplies a special knitting around the template, while monomer supplies specific or selective binding sites. Addition of template molecule during the polymerization is the key point for MIP

preparation. Template molecule should not have any functional group that stop or retard the polymerization and should be stable in a wide range of temperature and UV-radiation.

There are three basic steps in the synthesis of molecular imprinted polymers (Figure 1.5)

In pre-polymerization step, monomer and template molecule are let to connect to each other via covalent or non-covalent interaction. These interactions determine the imprinting type and specific name of the total process, semi-covalent imprinting or non-covalent imprinting. Non-covalent approach is based on polar interactions such as H-bonding and electrostatic interactions. Semi-covalent imprinting occurs from covalent bonding in which covalent bonds are formed during the pre-polymerization step, but rebinding is achieved by non-covalent approach again (Fontanals et al., 2010). The non-covalent approach is generally preferred due to the fast removal, rebinding, and release of template. However, restricted conditions during polymerization make non-covalent imprinting not an easy process at the beginning (Komiyama et al., 2003).

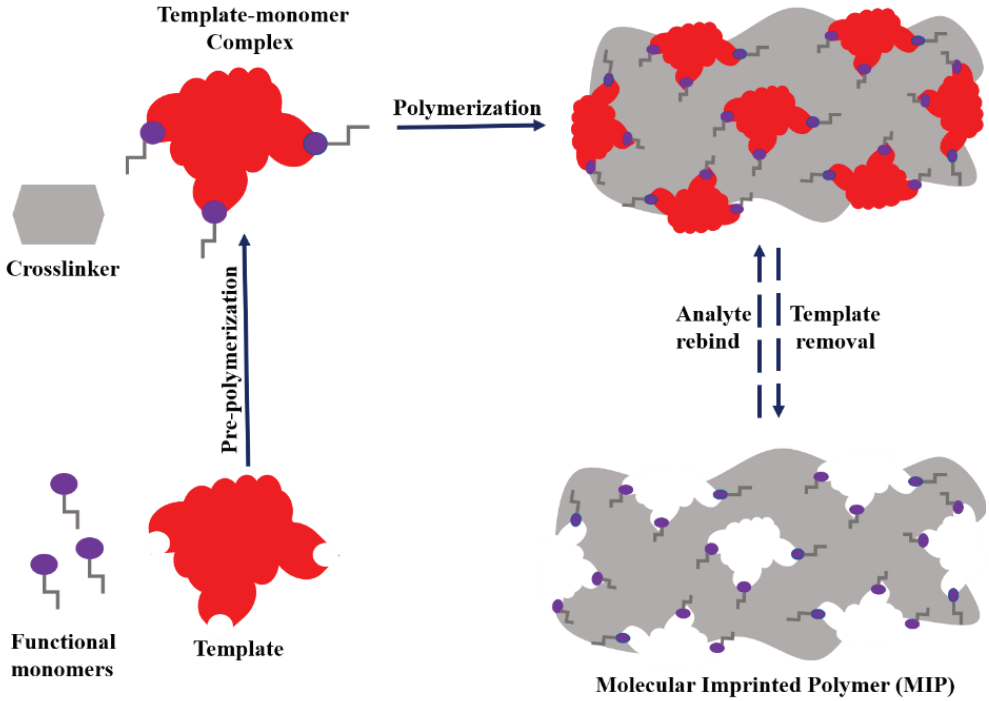

Figure 1.5. Schematic illustration of molecular imprinting.

The type of the solvent that polymerization takes place determines the type of imprinting process. Two types of solvents may be used during polymerization: nonpolar to moderately polar/aprotic solvents/porogens (DCM, toluene, chloroform, acetonitrile)

and polar protic solvents (methanol, ethanol, water). Polar protic solvents decrease the polarity of the interactions between the template and monomer, so they are used for covalent imprinting. In contrast to protic solvents, aprotic solvents (porogens) support and stabilize the H-bonding during non-covalent interaction (Fontanals et al., 2010).

In the polymerization step, crosslinking agent and initiator are added into the reaction mixture with a fixed ratio and the mixture is left to polymerize. Crosslinking agent controls the morphology of MIP and supplies robustness to the polymer while stabilizing the specific binding sites (imprinted region). The addition of initiator under proper conditions changes the route of polymerization step if radical copolymerization method is chosen. Free radical copolymerization is initiated by the thermal decomposition of radical initiator and molecular oxygen is taken away from the reaction mixture in order to prevent from trapping of radical. Oxygen is removed by degassing with argon or nitrogen gas or freeze-and-thaw cycle. In some cases, application of high temperatures for initiation can be harmful to non-covalent interaction between monomer and template. This time photo-initiation by UV light can be applied under low temperatures. In addition to these, the usage of UV-absorbable monomer supplies the initiation in the absence of initiator. If these processes are not applied, the polymerization cannot be started (Komiyama et al., 2003).

After the achievement of polymerization, the solid particles, now called MIPs, are filtered, then washed until no template molecule is observed at any detection method. If the analyte molecule used as the template is not washed out completely during the template removal step, an undesired phenomenon, so-called template bleeding occurs and affects the results especially in trace analysis. A dummy molecule can be used as template to overcome this problem. Dummy molecules should resemble the target analyte in terms of size, shape and functionality, but gives different chromatographic separation than template. Thereby, template and analyte molecule can be discriminated during chromatographic separation (Fontanals et al., 2010).

Addition of the template molecule during polymerization supplies specificity or selectivity to polymer by creating imprinted sites for the analyte or analyte group. To understand the existence of imprinted sites, an extra polymer is synthesized under the same conditions as MIP. However, this time template or dummy molecule is not added into the reaction medium, means that imprinted sites are not created. This second substance is called Non-Imprinted Polymer (NIP) and can be considered as the ‘sorbent

blank' or 'control sorbent'. By comparing the results of MIP and NIP, selectivity can be clarified.

1.2.1.2. Sorption Isotherm Models

Sorption isotherms describe the retention of substance on an adsorbent for different concentrations at constant temperature. Prediction of the mobility of a substance can be predicted by using the models. Up to now fifteen different isotherm model is described (*Adsorption*, 2022). In this thesis, the applicability of Langmuir, Freundlich, and Dubinin Radushkevich (D-R) isotherm models to the sorption data will be tested.

1.2.1.2.1. Langmuir Isotherm

Langmuir isotherm assumes that the energy of sorption is constant. Sorption occurs at well-defined homogenous sites and monolayer coverage occurs. The non-linear form of the isotherm is given in Equation 2.

$$Qe = Qmax \times \frac{bCe}{1+bCe} \qquad \text{Equation 2}$$

Here Q_e is the amount of the analyte adsorbed on the surface of the sorbent (mmol/g). Q_{max} amount of analyte sorption corresponding to monolayer coverage (mmol/g). C_e is the amount of analyte in liquid phase at equilibrium (mmol/L) and b is the affinity of analyte for sorbent. The constants Q_{max} and b can be evaluated from the linearized form of Equation 2 and by plotting $1/Q_e$ versus $1/C_e$ in Equation 3 (Boyaci et al., 2010; Limousin et al., 2007)

$$\frac{1}{Qe} = \frac{1}{Qmax} + \frac{1}{QmaxbCe} \qquad \text{Equation 3}$$

1.2.1.2.2. Freundlich Isotherm

As most widely used isotherm, Freundlich isotherm can be used for the heterogeneous surfaces over wide range of concentrations. The nonlinear form of the isotherm is given in Equation 4.

$$Qe = K_F \times Ce^{1/n} \qquad \text{Equation 4}$$

K_F (maximum absorption capacity) and n are constants and can be evaluated from the linear form of Equation 4 and by plotting $\log Q_e$ versus $\log C_e$ in Equation 5 (Boyaci et al., 2010; Limousin et al., 2007).

$$logQe = \log K_F + \frac{1}{n} logCe \qquad \text{Equation 5}$$

1.2.1.2.3. Dubinin Radushkevich Isotherm

D-R isotherm model uses the assumption that the species preferently bind to the most energetically favorable sites on the sorbent. The D-R model formulation is given in Equation 6.

$$Qe = qs \times \exp(-B\varepsilon^2) \qquad \text{Equation 6}$$

B gives information about the energy required to transfer one mole of analyte to the surface of the solid from infinity in the solution, q_s corresponds to the sorption monolayer capacity and ε is given in Equation 7.

$$\varepsilon = RTln(1 + \frac{1}{Ce}) \qquad \text{Equation 7}$$

Also mean free energy of sorption E, can be calculated using B (Equation 8).

$$E = (2B)^{1/2} \qquad \text{Equation 8}$$

In general, q_s and B constants can be obtained by plotting ln Q_e versus ε^2 (Boyaci et al., 2010; Limousin et al., 2007).

1.3. Electroanalytical Methods

In an electrochemical method, the electrical stimulation is used to analyze the chemical reactivity of a solution or a surface. Generally, an electrode is immersed in an electrolyte to control the rate of oxidation/reduction rates by a potentiostat (Westbroek, 2005). Electroanalytical methods are about the study of an analyte in an electrochemical cell by measuring the potential or current.

Electroanalytical methods can be classified as potentiometry, coulometry, voltammetry and electrochemical impedance spectroscopy (EIS). Potentiometry measures the difference between electrode potentials (volts, V). It uses two electrodes, reference and indicator electrode. Reference electrode has a constant potential. Indicator electrode potential changes depend on composition/concentration of sample solution. The indicator electrode is generally made sensitive to analyte of interest. This method is non-destructive and assumes that the electrode is in equilibrium with the solution. Coulometry measures the cell current over time (amperes, A). The current is used to determine the number of electrons passed. Also this can be used to determine the analyte concentration or the number of electron transfer during redox reaction for known concentrations. Voltammetry measures the cell current while actively altering the cell potential. In this method constant or varying potentials can be applied. It uses three electrode systems, working electrode (WE), reference electrode (RE) and counter electrode (CE). Chemically modified working electrodes can be used to analyze organic or inorganic analytes (*Electroanalytical methods*, 2022). In this thesis cyclic voltammetry (CV) will be used to modify the working electrode surface. Molecular imprinted polymer and corresponding non-imprinted polymer will be electrochemically synthesized on the surface of working electrode by cyclic voltammetry.

1.3.1. Cyclic Voltammetry

Cyclic voltammetry (CV) is a potentiodynamic electrochemical measurement in which working electrode (WE) is exposed to a ramped voltage over time. The voltage is measured between WE and the reference electrode (RE). During this time the current is also measured between WE and counter electrode (CE). The system which consist of WE, RE, CE and electrolyte is called an electrochemical cell (Figure 1.6).

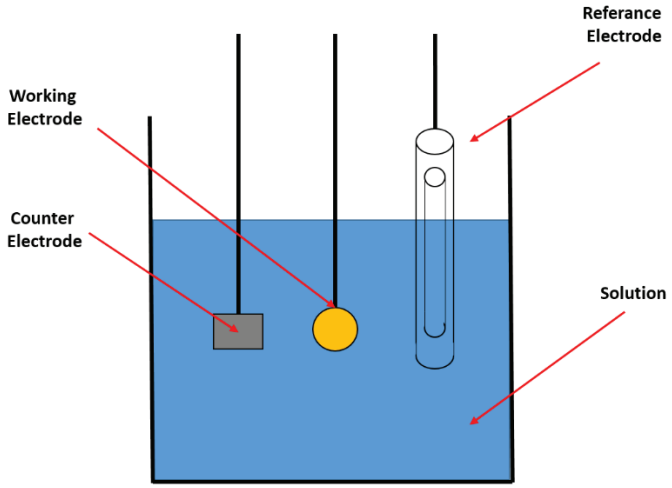

Figure 1.6. Schematic representation of an electrochemical cell.

After the pre-defined voltage is reached, opposite direction ramped voltage is applied. This cycle can be applied as needed. At the end of the cycles, a voltammogram is obtained that shows the current against the applied voltage. Figure 1.7 shows a typical voltammogram of polyaniline (PANI) film formation.

Cyclic voltammetry is generally used to reveal the electrochemical properties of an analyte in solution or a molecule that absorbed on the surface of an electrode. The voltammogram generally shows a reversible or irreversible redox reaction. It can be also used for electropolymerization of a monomer on WE.

Monomers to be used in electropolymerization should be selected carefully. The characteristics of electrical conductivity of the monomers is the determinative property. The most widely used monomers are aniline (ANI) and pyrrole (PYR), which attract attention due to their electropolymerizability and doping, dedoping or redox properties thanks to their conjugated structures (Figure 1.8) (Apodaca et al., 2011). Also 4-vinylpyridine (4-VP) with aromatic pyridine ring and alkene moiety is a good option for poly(4-vinylpyridine) electropolymerization. The 4-VP monomer is resistant to chemical

and physical damage. It has high electrical conductivity and good redox potential (Munawar et al., 2020).

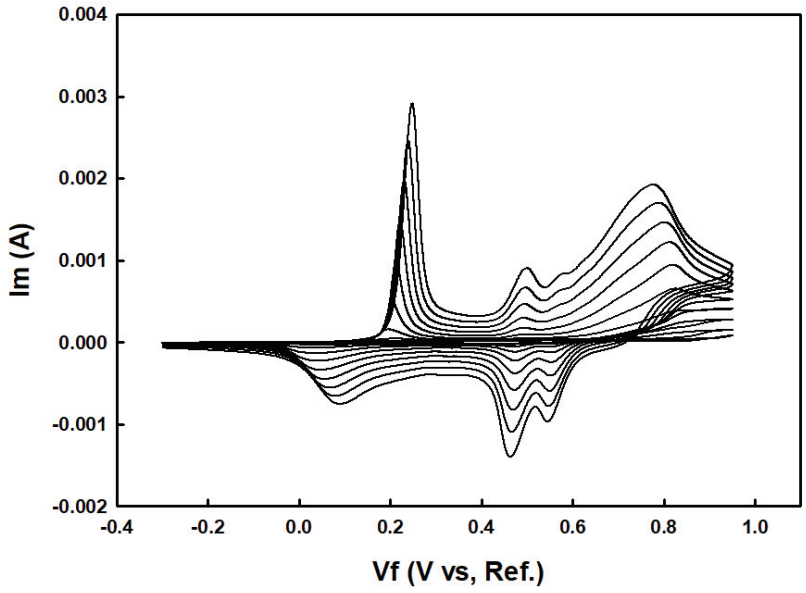

Figure 1.7. Typical voltammogram of polyaniline film formation obtained by cyclic voltammetry.

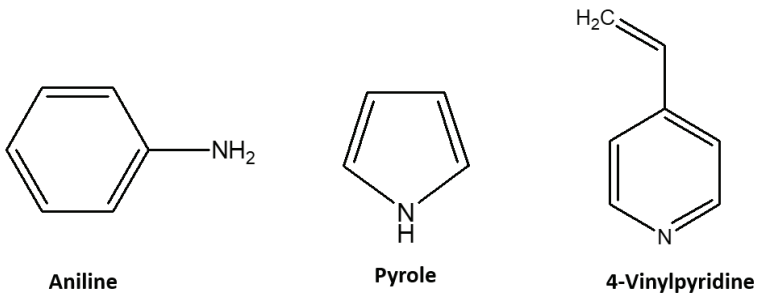

Figure 1.8. Chemical structures of aniline, pyrole and 4-vinylpyridine.

In case of molecular imprinting, electrochemical polymerization of a monomer supplies some advantages over other methods like bulk polymerization, precipitation polymerization or multi-step swelling. The most important of these is the ability to easily control the film thickness and the accessibility of specific or selective analyte cavities created in MIP. If it is considered that the sorption in molecular imprinting is achieved by mass transfer, these thin films, which were prepared in a controlled and open manner, can show sorption differences even at low concentrations (Apodaca et al., 2011). In the synthesis of electropolymerized MIP/NIP films, the crosslinker, that is used in other polymerization methods, is not used. Thus, non-specific or non-selective surface

sorptions are deactivated (Munawar et al., 2020). This can make the difference between MIP/NIP clearer.

1.3.2. Electrochemical Impedance Spectroscopy

Electrochemical impedance spectroscopy (EIS) is a powerful electrochemical method that can be used to understand the bio-recognition events by analyzing the interfacial properties occurring on an electrode surface (Magar et al., 2021).

In general, diagnostic purposes are related to the characterization of changes at a surface when exposed to reactive media under defined conditions. However, these processes change electrochemical dynamics which are extremely non-linear. As application purposes, controlled system parameters may be used to obtain desirable effect on surface. These two purposes can be examined by EIS in which the response of an electrochemical system to an applied voltage is obtained. The frequency dependence of this measurement can be used to unravel the non-linear processes.

In general, electrode and analyte interactions in an electrochemical cell are analyzed in terms of amount of the electroactive species, mass transfer and charge transfer. Also the resistance of the electrolyte solution containing the analyte is considered. The characterization is made by electrical circuits containing constant phase elements, capacitors and resistance. In addition to charge and mass transfer, EIS also analyzes the diffusion processes. The technique is used to understand the material properties that also have influences on resistivity, conductivity and capacitance of a system. Impedance, like resistance, is the ability of the system to resist the flow of current. Unlike the resistance, it does not follow the Ohm's Law used in direct current (DC) circuits. The usage of Ohm's Law is limited only for one circuit element, namely ideal resistor. For simplification, this resistor considered as that it obeys the Ohm's Law at all currents and voltages, independent of frequency. Also it is accepted that the alternating current (AC) and voltage are in phase with each other. In an EIS measurement, the impedance is measured by applying a small excitation signal. The response of the system is pseudo-linear. A phase shift occurs in sinusoidal current response to sinusoidal potential (Figure 1.9).

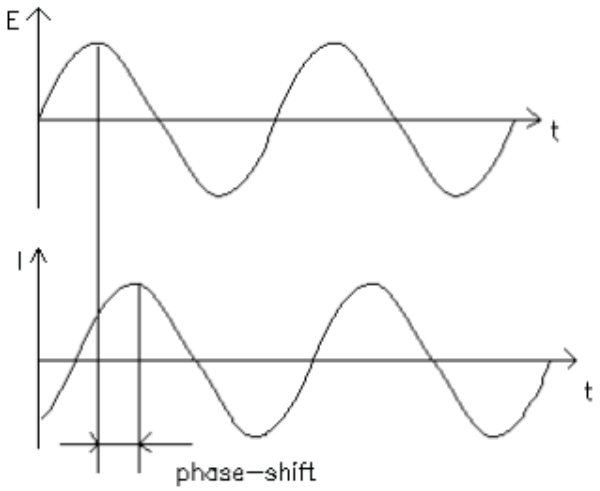

Figure 1.9. Sinusodial current response in a linear system.

Source: (Basics of Electrochemical Impedance Spectroscopy, 2022)

The time dependent excitation signal is given in Equation 9.

$$E_t = E_0 \sin(\omega t) \qquad \text{Equation 9}$$

Where E_t is the potential at time t, E_0 is the amplitude of signal at t_0, and ω is the radial frequency. The relation between radial frequency and applied frequency are given in Equation 10.

$$\omega = 2\pi f \qquad \text{Equation 10}$$

In linear system, the signal is shifted in phase Φ and has a different amplitude than I_0 (Equation 11).

$$I_t = I_0 \sin(\omega t + \Phi) \qquad \text{Equation 11}$$

The impedance of the system analogous to Ohm's Law can be obtained as in Equation 12.

$$Z = {}^{E}/_{I} = Z_0 \exp(i\Phi) = Z_0(\cos\Phi + i\sin\Phi) \qquad \text{Equation 12}$$

Where the impedance, Z expressed as magnitude Z_0 and phase shift Φ. Before the modern EIS measurements, Lissajous analysis was achieved for impedance measurements by plotting sinusoidal applied signal on x-axis and sinusoidal response signal I on y-axis (Bahadır & Sezgintürk, 2016).

It is clear from Equation 12 that the impedance has a real (Z_{real}) and an imaginery (Z_{img}) part. If the Z_{real} plotted on the x-axis and the Z_{img} on y-axis, the Nyquist plot is obtained (Figure 1.10). In general, the semi-circle represents the charge transfer region and the straight line at right side represents the diffusion region. Every point in this plot belongs to different frequency impedance. The frequency decreases from left to right side. However, the frequency change cannot be obtained from the Nyquist plot. The Bode Plot is also used to show frequency response of the system against impedance, Z and phase shift Φ.

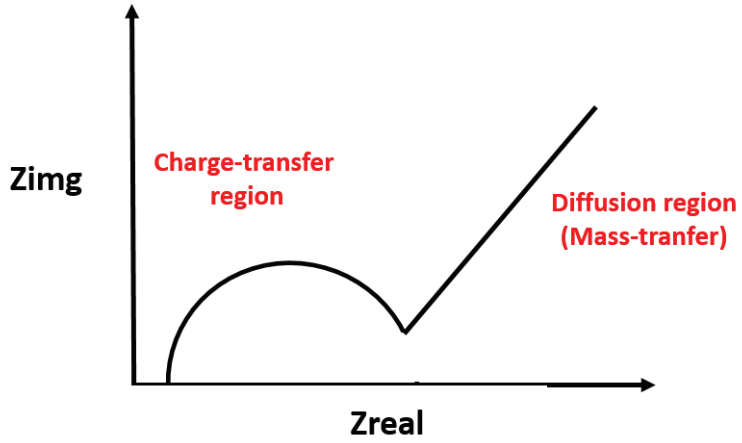

Figure 1.10. A typical Nyquist plot.

The EIS data can be analyzed by fitting the results to an equivalent electrical circuit. These circuits involve electrical components like resistance, capacitor and inductance. Equivalent circuits are used to understand and evaluate the EIS components. The mostly used equivalent circuit in literature is the Randles equivalent circuits (Figure 1.11). In this equivalent circuit solution resistance (R_s), double layer capacitance (C_{dl}), charge transfer resistance (R_{ct}) and Warburg resistance (W) are simplified (Magar et al., 2021). Solution resistance (R_s) represents the resistance of ionic solution used during analysis in a three electrode system. During modelling its effect should be considered for both between counter and reference electrode and reference and working electrode (*Basics of Electrochemical Impedance Spectroscopy*, 2022). Double layer capacitance (C_{dl}) occurs by the application of electricity to a system. It occurs when the electrolyte

solution and electrode are in touch with each other. The electrons are line up and the electricity is stored at the surface of electrode. In practice, perfect capacitor does not exist.

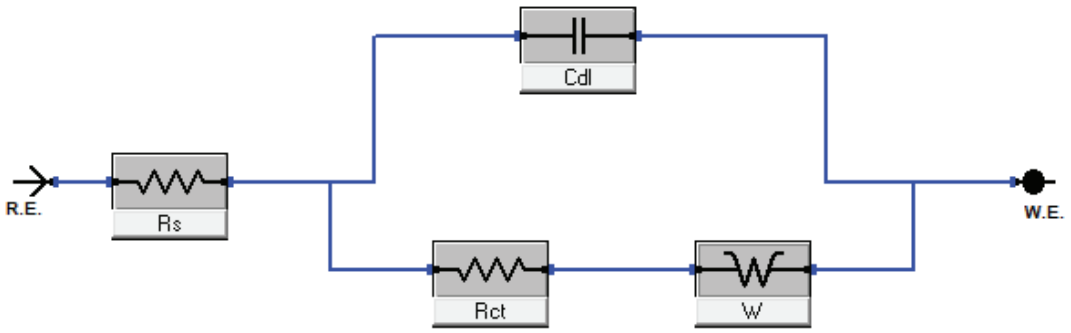

Figure 1.11. Randles equivalent circuit.

Constant phase element (CPE) can be taken into the consideration. It represents the surface roughness, non-homogenity and surface porosity (Sun and Liu, 2019). The charge transfer resistance (Rct) is like the electrical resistance. It represents the difficulty of the transfer of a charge from one component to another. Warburg resistance (Zw) occurs in case of diffusion. At high frequencies diffusing components cannot move very far, but at low frequencies, diffusion occurs farther and Warburg resistance occur. In Nyquist plot (Figure 1.10), Warburg resistance can be shown in right sight, at low frequency area. It exhibits a phase shift on bode plot higher than 45°.

Electrochemical impedance spectroscopy is generally used for the investigation of redox couples. Leuaa et al. (2020) modified the glassy carbon disk electrode/electrolyte interface with carbon. This modification is used to investigate the mass and charge transfer processes of VO^{2+}/VO^{2+} (V^{4+}/V^{5+}) redox species. They found that the electrolyte containing either V^{4+} or V^{5+} species showed a straight line capacitor feature by showing no oxidation-reduction. When the solution contained equal amount of V^{4+} and V^{5+} both charge transfer and mass transfer occurred at EIS pattern. There are also studies that working electrodes are modified with MIP/NIP and EIS technique was used to determine the coating performance against the analyte of interest. Khadro et al. (2010) modified the gold surface with MIP by solvent evaporation processing of poly(ethylene-co-vinyl alcohol) that is selective to creatinine and urea. EIS response showed a limit of detection (LOD) of 10 ng/mL with linear range from 0.02 µg/mL to 3 µg/mL for urea and 40 ng/mL of detection limit with linear range from 0.05 µg/mL to 2 µg/mL for creatinine. In another work, gold microelectrode was modified with MIP by electrodeposition of chitosan

biopolymer for the recognition of glyphosate [N-(phosphonomethyl) glycine] by EIS method. Label free detection of glyphosate was achieved with a linear plot ranging from 0.31 pg/ml to 50 ng/ml with a low LOD of 0.001 pg/ml (Zouaoui et al., 2020). In another work, Au electrode surface was modified with MIP for the aspirin detection. The MIP film was prepared by co-polymerization of p-aminothiophenol (p-ATP) and $HAuCl_4$. The prepared sensor was characterized by EIS, CV and differential pulse voltammetry (DPV). A linear relationship between current and logarithmic concentration were obtained in the range from 1 nmol/L to 0.1 μmol/L and 0.7 μmol/L to 0.1 mmol/L. The detection limit of 0.3 nmol/L was achieved (Wang et al., 2011).

1.4. Quartz Crystal Microbalance

The main aim of this study is to use QCM as a scales that can detect small amounts of vitamin D3 in sample solution. Quartz crystal microbalance is a powerful technique that can measure nanogram to microgram mass changes in mass per unit area. All the measurements are made by analyzing the oscillation frequency of the quartz crystal. The crystal is a piezoelectric material that can oscillate at a defined frequency by the application of a voltage. The oscillation frequency can change by molecular interactions (adsorption or removal of a mass) on the crystal surface, such as film formation, oxidation/reduction. The technique can be used under vacuum for the determination gaseous species or more recently for liquid samples to determine the affinity of the analyte of interest to a functionalized crystal surface.

The technique uses the piezoelectric properties of quartz crystal. Piezoelectricity of a crystal is explained by the ability of turning the mechanical energy into an electrical field. The mechanical energy is supplied by the applied pressure. The advantages of quartz over other piezoelectric materials are low resistance to the propagation of acoustic waves, high shear modulus and being chemically stable.

The application of an AC electrical field at a defined frequency makes the quartz vibrate in thickness shear mode. It moves with the same amplitude in opposite direction as represented in Figure 1.12.

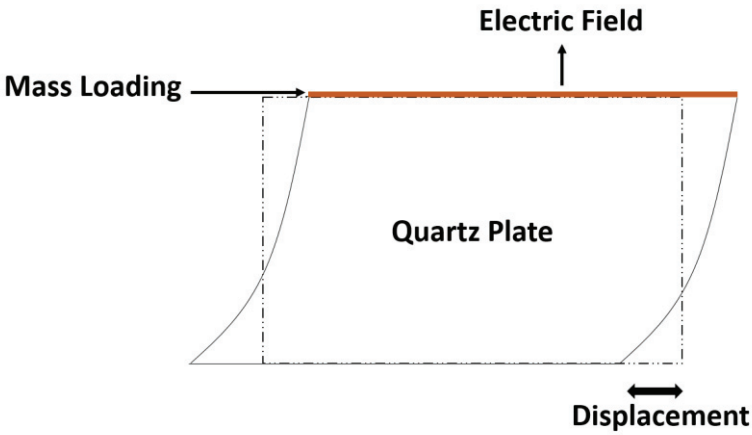

Figure 1.12. Thickness shear mode of Quartz Crystal Microbalance

The maximum amplitude of displacement is obtained at the resonance frequency and is given in Equation 13.

$$\frac{n\lambda_0}{2} = d \qquad \text{Equation 13}$$

Where n is the harmonic mode, λ_0 is the wavelength of the acoustic wave in 1/m and d is the crystal plate thickness. Also the wavelength λ_0 is related to the resonance frequency f_0 and the shear or tangential velocity of the crystal in m/s, V_c and given in Equation 14.

$$\lambda_0 = \frac{f_0}{v_c} \qquad \text{Equation 14}$$

By the combination of Equation 13 and Equation 14 resonance frequency, f_0, now can be expressed as in Equation 15.

$$f_0 = \frac{V_c}{2d} \qquad \text{Equation 15}$$

The quartz crystal is generally coated (usually with gold) on both sides with an electrically conducting material (electrode). Chromium or titanium can be used as an adhesion layer between the crystal and the electrode. Titanium is more preferred because it contaminates Au twice less compared to Cr (Hoogvliet & van Bennekom, 2001). When the Au coated quartz is exposed to an AC voltage, two parallel electrodes and quartz

vibrates assuming that Au electrodes and quartz moving at the same speed and also acoustic wave propagation occurs at the same speed in the metallic (Au) electrodes and quartz. Sauerbey equation, given in Equation 16, expresses the relationship between the mass change and the resonance frequency change by expressing Δf_n, the change of resonance frequency at the n^{th} harmonic in Hz (Sauerbrey, 1959).

$$\Delta f_n = -n \frac{2 f_{0,n}{}^2}{\sqrt{\mu_q \rho_q}} \Delta m_a \qquad \text{Equation 16}$$

where n is the harmonic order, $f_{0,n}$ is the resonant frequency at the nth harmonic in Hz, μ_q is the shear elastic modulus of the quartz in kg/ms or Pas, ρ_q is the quartz density in kg/m^3, and Δm_a is the mass of the film in kg/m^2.

The Sauerbey equation is used to define the mass or thickness change of the rigid layer deposited on Au electrode surface (Figure 1.13). The wave propagates at the same speed with film, Au electrode and quartz. According to Sauerbey equation, an increase in the film thickness will change the resonance frequency, f_0.

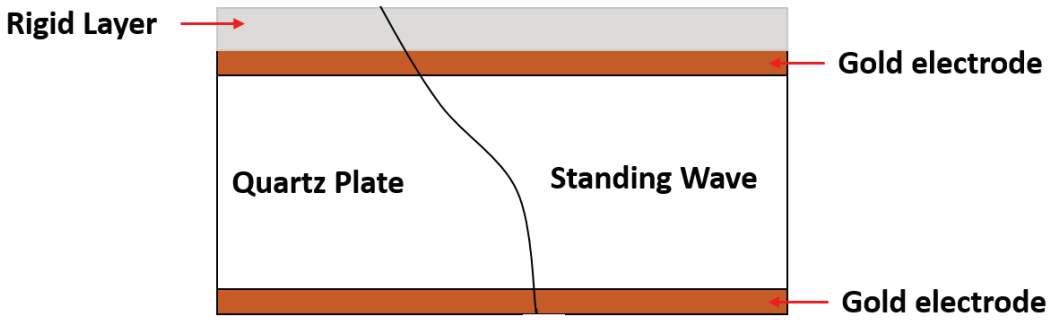

Figure 1.13. Acoustic standing wave across the sensor with a rigid layer.

Electrochemical quartz crystal microbalance (eQCM) can be thought as the combination of electrochemisty and QCM. It contains an electrochemical cell and QCM part. The both sided coated Au electrode on quartz crystal serve as both alternating electric field generation for making up the oscillator (QCM part) and WE together with CE and RE as in an electrochemical cell (Bruckenstein & Shay, 1985; Streinz et al., 1995). eQCM can be used in electrosynthesis for monitoring the chemical reactions occurring on electrode (Baker et al., 1991; Chung et al., 1997; Wei et al., 2018). By this way polymerization can be achieved on Au coated quartz crystal. It also can be used for electrodeposition/dissolution (Bohannan et al., 1999), adsorption/desorption (Kawaguchi

et al., 2000; Schneider & Buttry, 1993), the usage of polymer modified electrodes (Zotti et al., 1995) and energy conversion/storage (Levi et al., 2009).

In this thesis, eQCM method will be used for the electrochemical synthesis of poly(4-vinylpyridine) on gold coated quartz crystal for the detection of vitamin D3. The parameters optimized during the CV process will be used during the electrosynthesis. Than the QCM will be used as a scales to determine the amount of vitamin D3 in different concentrations.

In literature, there are studies that uses the eQCM method for coating the quartz crystal, then QCM is used for determinations. Kumar Singh and Singh (2015) used eQCM method for electropolymerization of 3-thiophene acetic acid for the determination of melphalan. Molecular imprinted film was also electropolymerized in the presence of melphalan. They used QCM to verify the changes in currents (Kushwaha et al., 2022). They concluded that highly sensitive and selective piezoelectric sensor for melphalan has been reported. In another work, S-cathinone imprinted polymer nanoparticles were deposited on gold coated quartz crystal electrode of eQCM. The authors concluded that the fabricated sensor was able to discriminate between stereoisomers and other structurally related compounds. The reported LOD was 0.12 ng/mL and LOQ was 0.409 ng/mL. Liu et al. (2006) fabricated thin permeable films MIP on QCM surface by using acrylamide and trimethylolpropane trimethacrylate as a functional monomer and a cross-linking agent providing enantioselectivity to tryptophan enantiomers. The detection limit was found as 8.8 μM. In another work, molecularly imprinted polypeptide gel layers based on cyclodextrin-modified poly(L-lysine) on quartz crystal microbalance (QCM) sensor chips were prepared for the determination of bisphenol A (Matsumoto et al., 2016). The gel layer is prepared on electropolymerized polyterthiophene films that are formed by eQCM. This work is a good example of combination of in situ electropolymerization using eQCM and molecular imprinting.

CHAPTER 2

DETERMINATION OF VITAMIN D3 BY SOLID PHASE EXTRACTION PRIOR TO HPLC ANALYSIS

2.1. Aim of the Study

The main aim of this section is to prepare MIP/NIP solid phase extraction sorbents for the recognition of vitamin D3 prior to chromatographic determination. The sorption performances of the sorbents were investigated in terms of selectivity and other analytical performance figures. Based on the initial performances of the sorbents, one of the MIPs was chosen for further studies. Afterwards, optimization parameters of the proposed procedure were examined in terms of sorption time, amount of sorbent, volume of working solution and eluent type. Validation studies were performed by spiking vitamin D3 in phosphate buffered saline (PBS) solution.

2.2. Experimental

2.2.1. Chemicals and Reagents

All chemicals and reagents were analytical grade. Cholecalciferol (vitamin D3), ergocalciferol (vitamin D2), 25-hydroxycholecalciferol (25(OH)D3) and vitamin K1 were obtained from Sigma Aldrich. Stock solutions (500.0 mg/L) were prepared in methanol as monthly in amber bottles and stored at –20 °C in freezer. All studied solutions were prepared daily by appropriate dilution of the stock solution. Doubly distilled ultra-pure water was used in all experiments. All solutions were filtered through 0.2 μm cellulose acetate or 0.2 μm polyamide membrane filters depending on the solvent system and degassed for 15 min in ultrasonic bath prior to HPLC analysis. In the synthesis of D3

imprinted polymer, methacrylic acid (MAA, ≥99%, Sigma Aldrich), or 4-vinylpyridine (4-VP, 95%, Sigma Aldrich) or (3-aminopropyl)trimethoxysilane (APTMS, 95%, Sigma Aldrich) or acrylamide (AA, 95%, Sigma Aldrich) were used as funtional monomer; trimethylolpropane trimethacrylate (TRIM, Aldrich) or ethyleneglycol dimethacrylate (EGDMA, 95%, Sigma Aldrich) or tetraethyl orthosilicate (TEOS, 95%, Sigma Aldrich) as crosslinker; HPLC grade acetonitrile (Sigma Aldrich) as porogen and 2,2' azobis(2,4-dimethyl valeronitrile (AIVN, Alfa Aesar) as initiator. The other solvents used through the study were all HPLC grade. For the preparation of PBS solution at pH 7.4, sodium chloride (NaCl, ACS reagent, ≥99%, Sigma Aldrich), potassium chloride (KCl, ACS reagent, 99.0-100.5%, Sigma Aldrich), sodium phosphate dibasic (Na_2HPO_4, ACS reagent, ≥99.0%, Sigma Aldrich) and potassium phosphate monobasic (KH_2PO_4 ACS reagent, ≥99.0%, Sigma Aldrich) were used.

2.2.2. Instrumentation

All analyses were performed with Agilent 1200 series HPLC with Diode Array Detector. The tested parameters are given in Table 2.1. After optimization of the experimental parameters, limit of detection (LOD) and limit of quantification (LOQ) were calculated by analyzing the least concentrated standard 10 times with HPLC-DAD. Three different columns were used during the HPLC-UV analysis; YMC Carotenoid C30 column (250 mm length× 4.6 mm I.D., 5 µm particle size), Waters Sunfire C18 column (250 mm length× 4.6 mm I.D., 5 µm particle size) and Eclipse XDB-C18 (250 mm length× 4.6 mm I.D., 5 µm particle size).

Table 2.1. Tested parameters for HPLC-DAD

	Mobile phase	Flow rate, mL/min	Column temperature, °C
C30 YMC Carotenoid 250 × 4.6 mm I.D., 5µm	100% MeOH MeOH:H_20 (99:1) MeOH:THF (gradient)	0.8, 1.0, 1.3	25.0, 30.0
C18 (WC18) Waters Sunfire C18 4.6 × 250 mm I.D., 5µm	MeOH:H_20 (80:20) (pH3, HOAc) 100% MeOH	0.7, 0.8, 0.9, 1.3, 1.5	25.0, 30.0, 35.0, 40.0
C18 (EC18) Eclipse XDB-C18 4.6 × 150 mm I.D., 5µm	MeOH:THF:H_2O (80:20:10) MeOH:THF (70:30) MeOH:THF (80:20) MeOH:THF (85:15) MeOH:THF (90:10) MeOH:THF (95:5) 100% MeOH	0.5, 0.6, 0.7, 0.8	25.0, 30.0

2.2.3. Synthesis of molecularly imprinted (and non-imprinted) polymers (MIPs and NIPs)

Molecularly imprinted and non-imprinted polymers should be prepared parallel and in an identical way. During the synthesis of MIP three different strategies were used for polymerization; namely, precipitation polymerization for organic MIP/NIP synthesis, inorganic MIP/NIP synthesis and sol-gel method.

For precipitation polymerization (organic MIP/NIP), the same steps were followed for different template molecules, monomers, cross-linkers and their ratios as given in Table 2.2. Firstly, template molecule, monomer and porogen were added into an amber reaction vessel and stirred 1.0 hour for pre-polymerization; then, cross-linker was added. Initiator was used % 2 mole of all reagents except template molecule in reaction mixture and was added under Ar gas carefully to remove dissolved oxygen. Polymerization reaction was performed in an oil bath at 60°C, 8 hours.

After polymerization, solid MIP was obtained. Removal of template molecule was performed by using methanol (MeOH). After complete removal of the template molecule, MIPs were dried in an oven at 60.0 °C and the sorbent was ready for the experiments. The preparation of NIP was the same as in MIP except the addition of template. Effect of

different template, monomer, cross-linker and mixing ratios was investigated (Table 2.2). In the table, batch no.s 1-8 belong to the organic MIP/NIP synthesized by the precipitation method as explained above.

Table 2.2. Template molecule, monomer, crosslinker, ratios and solvents used in synthesis.

Batch no.		**Template/Dummy Molecule**	**Monomer**	**Cross-linker**	**Ratio**	**Solvent**	**Solvent Amount**
1	MIP1	D3	MAA	TRIM	01:02:10	ACN	100 mL
	NIP1	-	MAA	TRIM	00:02:10	ACN	100 mL
2	MIP2	D3	MAA	TRIM	01:02:20	ACN	100 mL
	NIP2	-	MAA	TRIM	00:02:20	ACN	100 mL
3	MIP3	D3	MAA	TRIM	01:02:20	DMF	100 mL
	NIP3	-	MAA	TRIM	00:02:20	DMF	100 mL
4	MIP4	D3	MAA	TRIM	01:08:20	ACN	100 mL
	NIP4	-	MAA	TRIM	00:08:20	ACN	100 mL
5	MIP5	D3	MAA	TRIM	01:16:25	CH	100 mL
	NIP5	-	MAA	TRIM	00:16:25	CH	100 mL
6	MIP6	D2	MAA	TRIM	01:08:20	ACN	100 mL
	NIP6	-	MAA	TRIM	00:08:20	ACN	100 mL
7	MIP7	7-DHC	AA	TRIM	01:08:20	ACN	100 mL
	NIP7	-	AA	TRIM	00:08:20	ACN	100 mL
8	MIP8	7-DHC	4-VP	EGDMA	01:06:30	ACN	100 mL
	NIP8	-	4-VP	EGDMA	01:06:30	ACN	100 mL
9	MIIP	7-DHC	APTMS	TEOS	01:08:20	THF:H_2O	100 mL
	NIIP	-	APMTS	TEOS	00:08:20	THF:H_2O	100 mL
10	MIPS	D3, D2, 7-DHC	MAA	TEOS & EGDMA	01:08:20	EtOH	4.5 mL
	NIPS	-	MAA	TEOS & EGDMA	01:08:20	EtOH	4.5 mL

The schematic representation of MIP synthesis in which 7-dehydrocholesterol was used as the dummy template molecule, 4-VP as monomer and EGDMA as crosslinker is given in Figure 2.1. This scheme can also be used to show the basic steps of precipitation polymerization applied during the studies. NIP synthesis by precipitation polymerization was achieved via the same way, except the addition of the template molecule.

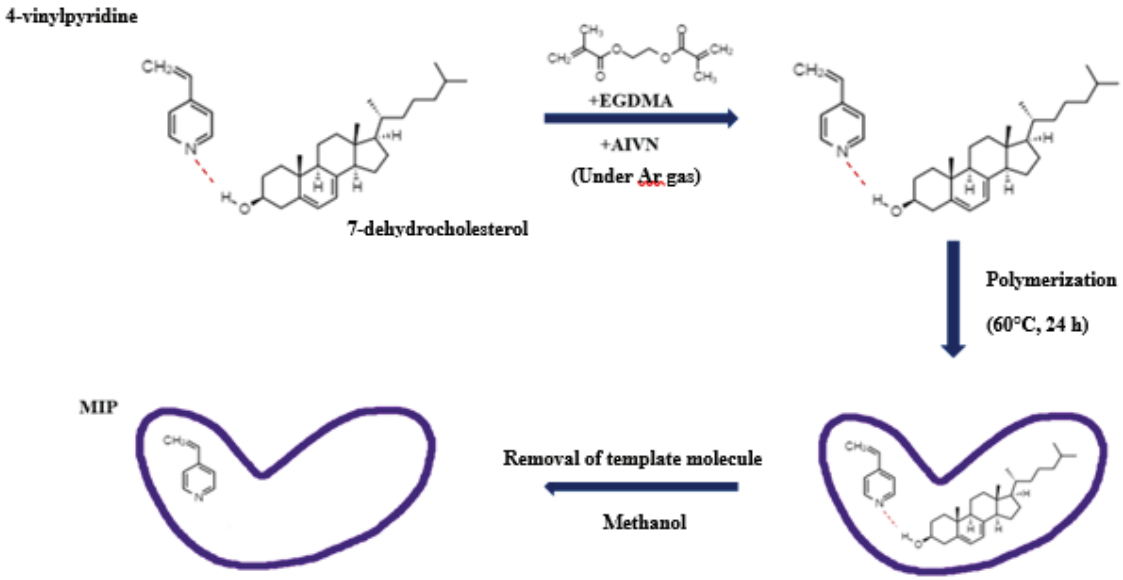

Figure 2.1. Schematic representation of MIP synthesis in which 7-dehydrocholesterol was used as dummy template dummy molecule, 4-VP as monomer and EGDMA as crosslinker.

In molecular imprinted inorganic polymers and non-imprinted inorganic polymers (MIIP/NIIP), same synthesis route as in organic precipitation procedure were followed except for the application of heat.

MIPS/NIPS were synthesized by sol-gel method. Firstly, two different solutions were prepared. In one solution template molecule and TEOS were let to make –OH bonds. In another solution MAA and EGDMA were mixed at 60°C. After that, the two solutions were mixed and polymerization reaction was performed in an oil bath at 50.0°C for 1 hour. After complete removal of template molecule, MIPs/NIPs were dried in an oven at 60.0 °C for 48 hours.

The MIP/NIP couple showing the better selectivity to vitamin D3 was characterized by scanning electron microscopy (SEM) and Brunauer-Emmett-Teller (BET) surface area analysis.

2.2.4. Binding Characteristic Assay

Binding characteristic assays experiments were firstly applied for MIP1 and NIP1. The reason was to determine the proper sorption solvent during the experiments due to the limited solubility of vitamin D derivatives in water.

Firstly, sample solutions were prepared in MeOH at vitamin D3 concentrations of 1.0, 5.0 and 10.0 mg/L. 10.0 mL of these solutions were taken into amber vials, which already had 10.0 mg of the sorbent MIP1 or NIP1. After that, mixtures were shaken at 50 rpm for 24 hours. The solid/liquid mixture was filtered through cellulose acetate membrane (0.2 μm pore size) to separate MIP1/NIP2 from solutions. Effluents were analyzed with HPLC-DAD at 264 and 220 nm.

Secondly the same procedure was applied using MIP1 and NIP1; but this time, sample solutions were prepared in ACN. This trial was only made for 1.0 mg/L of solution to avoid extravagance.

After that, H_2O:MeOH ratio of 90:10 (v/v) mixture was employed as the matrix for preparing sample solutions. The same procedure was applied to 1.0, 5.0, 10.0, 25.0 and 50.0 mg/L vitamin D3 concentrations.

Lastly, different ratios of H_2O:MeOH mixtures (95:5, 90:10 and 85:15, v/v) were tried for preparing sample solutions and the same sorption procedure was applied to 5.0 ppm of solutions.

By the help of above mentioned steps, H_2O:MeOH ratio of 90:10 (v/v) mixture was determined as the sorption solvent (sample matrix). The binding characteristic assay experiments were realized using this mixture as the sorption medium. For all syntheses this experiment was realized by using parameters as given in Table 2.3. Different concentrations of template molecules were mixed and shaken with the synthesized MIP and NIP in separate experiments. Effluents were analyzed with HPLC-DAD at 264 and 220 nm.

Table 2.3. Binding characteristics test parameters.

Standard concentrations	0.05, 0.10, 0.25, 0.50, 1.0 mg/L
Sorbent amount	10.0 mg
Volume of standard solutions	10.0 mL H_2O:MeOH 90:10 v/v
Sorption time	24 hours
Shaking speed	50 rpm
Reaction temperature	25.0 °C

Also the results of the binding characteristic assay experiments were used in sorption isotherms. Langmuir, Freundlich and Dubinin Radushkevich isotherm models were applied for the results with the formulations given in Section 1.2.1.2

2.2.5. Cross Sensitivity Experiments

In binding characteristics part, MIP8/NIP8 was chosen as the most suitable MIP/NIP by comparing the sorption performances against their corresponding template molecule. Cross-sensitivity experiments were made to determine whether the MIP8 is specific/selective to vitamin D3 or other molecules structurally similar to vitamin D3 or the sorbent shows no selectivity at all. For this purpose, sorption performance of MIP8/NIP8 were investigated in the presence of vitamin D3, vitamin D2, ergosterol, 7-dehydrocholesterol and vitamin K1. The experimental parameters are given in Table 2.4. Effluents were analyzed with HPLC-DAD at 264 and 220 nm.

Table 2.4. Sorption parameters of the cross-sensitivity experiment.

Standard concentration	1.0 mg/L
Sorbent amount	10.0 mg
Volume of standard solutions	10.0 mL (H_2O:MeOH 90:10 v/v)
Sorption time	24 hours
Shaking speed	50 rpm
Reaction temperature	25.0 °C

2.2.6. Effect of Sorption Time

10.0 mL of 1.0 mg/L vitamin D3 solution was added into sample vials containing 10.0 mg MIP8. Sorption was achieved by shaking at 50 rpm. Effluents were analyzed with HPLC-DAD at 264 and 220 nm after the mixture was filtered through cellulose acetate membranes (0.2 μm pore size) The test parameters are given in Table 2.5.

Table 2.5. Sorption time test parameters.

Standard concentration	1.0 mg/L
Sorbent amount	10.0 mg
Volume of standard solutions	10.0 mL H_2O:MeOH (90:10 v/v)
Sorption time	1 min. (manuel), 5 min., 30 min., 1 hour, 2 hours, 3 hours, 5 hours, 24 hours
Shaking speed	50 rpm
Reaction temperature	25.0 °C

2.2.7. Effect of Sorbent Amount

Effect of sorbent amount was investigated as follows; MIP8 sorbents were weighed as given in Table 2.6 and taken into amber vials. 10.0 mL of 1.0 mg/L vitamin D3 solution was added. Sorption was realized on the shaker at 50 rpm for 5 hours. Filtration was made with membrane filtration system by cellulose acetate membranes (0.2 μm pore size). Effluents were analyzed with HPLC-DAD at 264 and 220 nm.

Table 2.6. Studied parameters in sorbent amount determination.

Standard concentration	1.0 mg/L
Sorbent amount	5.0, 10.0, 25.0, 50.0 mg
Volume of standard solutions	10.0 mL H_2O:MeOH (90:10, v/v)
Sorption time	5 hours
Shaking speed	50 rpm
Reaction temperature	25.0 °C

2.2.8. Effect of Sample Volume

Sample volumes of vitamin D3 were prepared as in Table 2.7. 1.0 mg/L vitamin D3 solutions with different volumes were added into the sample vials containing 5.0 mg MIP8. Sorption was carried out on the shaker at 50 rpm for 5 hours. Membrane filtration system by cellulose acetate membranes (0.2 μm pore size) was used for filtration of the mixtures. Effluents were analyzed with HPLC-DAD at 264 and 220 nm.

Table 2.7. Optimization parameters for determination of sample volume.

Standard concentrations	1.0 mg/L
Sorbent amount	5.0 mg
Volume of standard solutions	1.0, 5.0, 10.0, 15.0 mL H_2O:MeOH (90:10, v/v)
Sorption time	5 hours
Shaking speed	50 rpm
Reaction temperature	25.0 °C

2.2.9. Sorption Performance: Comparison with Other Sorbents

The sorption process was applied to MIP8 and commercial hydrophilic/lipophilic balanced (HLB) and C30 sorbents. 5.0 mL of 1.0 mg/L vitamin D3 solutions were added into the sample vials containing 5.0 mg MIP8, HLB and C30. Sorption was carried out on the shaker at 50 rpm for 5 hours. Membrane filtration system by cellulose acetate membranes (0.2 μm pore size) was used for filtration of the mixtures. Effluents were analyzed with HPLC-DAD at 264 and 220 nm. Table 2.8 shows the experimental parameters employed.

Table 2.8. Parameters used in comparison with commercial sorbents.

Standard concentration	1.0 mg/L
Sorbent amount	5.0 mg
Sorbent Type	MIP8, NIP8, HLB and C30
Volume of standard solutions	5.0 mL H_2O:MeOH (90:10, v/v)
Sorption time	5 hours
Shaking speed	50 rpm
Reaction temperature	25.0 °C

2.2.10. Effect of Eluent Type

For the elution of Vitamin D3 from sorbent, three different candidate eluents were tried. 5.0 mL of 1.0 mg/L vitamin D3 solution were prepared and added into sample vials containing 5.0 mg of MIP8. Sorption was carried out on the shaker at 50 rpm for 5 hours. Membrane filtration system by cellulose acetate membranes (0.2 μm pore size) was used for filtration of the mixtures. After filtration, methanol (MeOH), methanol:water (MeOH:H_2O, 90:10 v/v) and methanol:acetic acid (MeOH:HOAc, 90:10 v/v) solutions were used as potential eluents. Effluents were analyzed with HPLC-DAD at 264 and 220 nm. Parameters used during the determination of eluent are given in Table 2.9.

Table 2.9. Parameters used in the determination of eluent type.

Standard concentration	1.0 mg/L
Sorbent amount	5.0 mg
Volume of standard solutions	5.0 mL H_2O:MeOH (90:10, v/v)
Sorption time	5 hours
Shaking speed	50 rpm
Reaction temperature	25.0 °C
Eluent volume and type	5.0 mL, MeOH, MeOH:H_2O (90:10, v/v), MeOH:HOAc (90:10, v/v)
Desorption Time	5 hours

2.2.11. Spike Recovery Tests

Sorption efficiency of sorbents was investigated by using spiked sample of H_2O:MeOH (90:10, v/v) and PBS:MeOH (90:10, v/v) (a mixture prepared by using phosphate buffer saline (PBS)). The PBS solution was used due to match of its osmolarity and ionic strength to human body. Spike recovery tests parameters are given in Table 2.10.

Table 2.10. Method validation parameters.

Standard concentration	1.0 mg/L
Sorbent amount	5.0 mg
Volume of standard solutions	5.0 mL in H_2O:MeOH (90:10, v/v) and PBS:MeOH (90:10, v/v)
Sorption time	5 hours
Shaking speed	50 rpm
Reaction temperature	25.0 °C
Eluent volume and type	5.0 mL, MeOH:HOAc (90:10, v/v)
Desorption Time	5 hours

2.2.12. Calibration Strategies

The suppression/enhancement effect of sample matrix, aqueous calibration and matrix-matched calibration strategies were investigated in such a way that different concentrations of vitamin D3 were prepared in both H_2O:MeOH (90:10, v/v) and PBS:MeOH (90:10, v/v) mixtures. Proposed SPE method was applied to these matrixes and the results were compared with the normal (aqueous) calibration without SPE method application. Matrix-matched calibration parameters are given in Table 2.11.

Table 2.11. Method Matrix Match Parameters.

Standard concentration	0.05, 0.10, 0.25, 0.50, 1.0 mg/L vitamin D3 in H_2O:MeOH (90:10, v/v) and PBS:MeOH (90:10, v/v)
Sorbent amount	5.0 mg
Volume of standard solutions	5.0 mL
Sorption time	5 hours
Shaking speed	50 rpm
Reaction temperature	25.0 °C
Eluent volume and type	5.0 mL, MeOH:HOAc 90:10 v/v
Desorption Time	5 hours

2.3. Results and Discussion

2.3.1. Instrumentation

Instrumental parameters given in Table 1.3 were used throughout the study. By using the WC18 column optimum parameters for mobile phase composition, flow rate, and column temperature were determined as 100% MeOH, 0.8 mL/min and 30ºC, respectively. LOD, LOQ, R^2 values and calibration line equations of vitamin D3 (D3), vitamin D2 (D2), ergosterol (ERG), 7-dehydrocholesterol (7-DHC) and Vitamin K1 (K1) were given in Table 2.11.

Table 2.11. LOD, LOQ, calibration line equations, R^2, wavelengths of analytes of interest.

	LOD (mg/L)	**LOQ (mg/L)**	**Equations**	**R^2**	**Wavelenghts (nm)**
D2	0.0208	0.0631	y= 52.541x - 0.659	0.9998	264
D3	0.0243	0.0736	y = 77.123x - 0.835	0.9997	264
ERG	0.0165	0.0501	y = 58.536x - 0.434	0.9999	280
7-DHC	0.0333	0.1008	y = 52.726x - 0.430	0.9996	280
K1	0.0386	0.1169	y = 30.550x - 0.618	0.9998	264

Calibration graphs for 7-deydrocholesterol, ergosterol, vitamin D3, vitamin D2 and vitamin K1with the use of optimum instrumental parameters is shown in Figure 2.2.

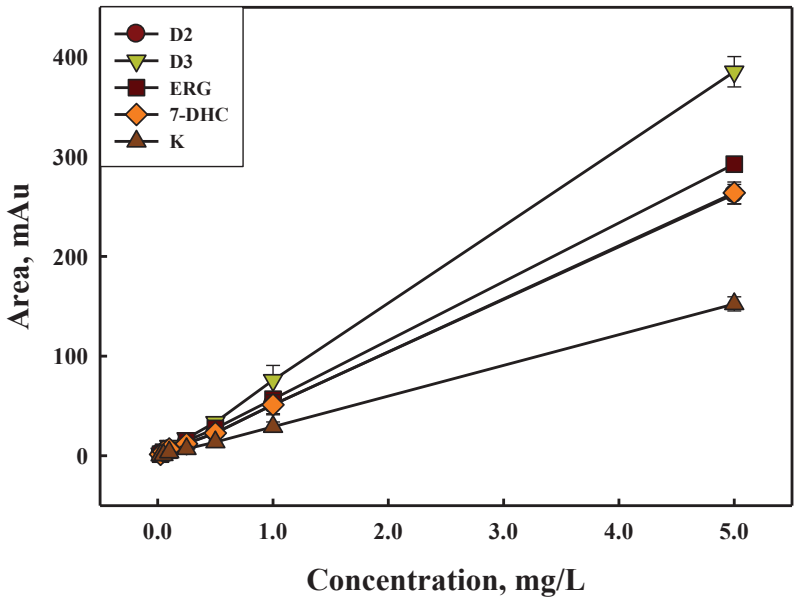

Figure 2.2. Calibration graph for 7-deydrocholesterol, ergosterol, vitamin D3, vitamin D2 and vitamin K1.

The separation of the vitamin D3 and vitamin D2 peaks cannot be achieved by using EC18 column. In Figure 2.3, the chromatogram obtained with WC18 column is given.

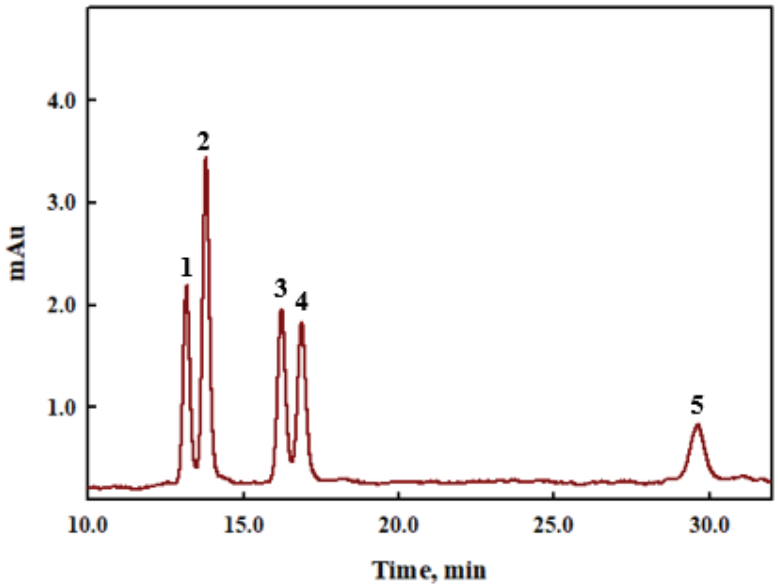

Figure 2.3. Chromatogram of a synthetic solution containing (1) vitamin D2, (2) vitamin D3, (3) ergosterol, (4) 7-dehydrocholesterol, (5) vitamin K.

2.3.2. Synthesis of molecularly imprinted (and non-imprinted) polymers (MIPs and NIPs)

Various types of MIPs and NIPs were synthesized using the methods given in Section 2.2.3, Table 3. Among the sorbents synthesized only MIP8/NIP8 showed a selectivity difference during binding characteristic assay. In Figure 2.4 SEM images of MIP8 and NIP8 is given.

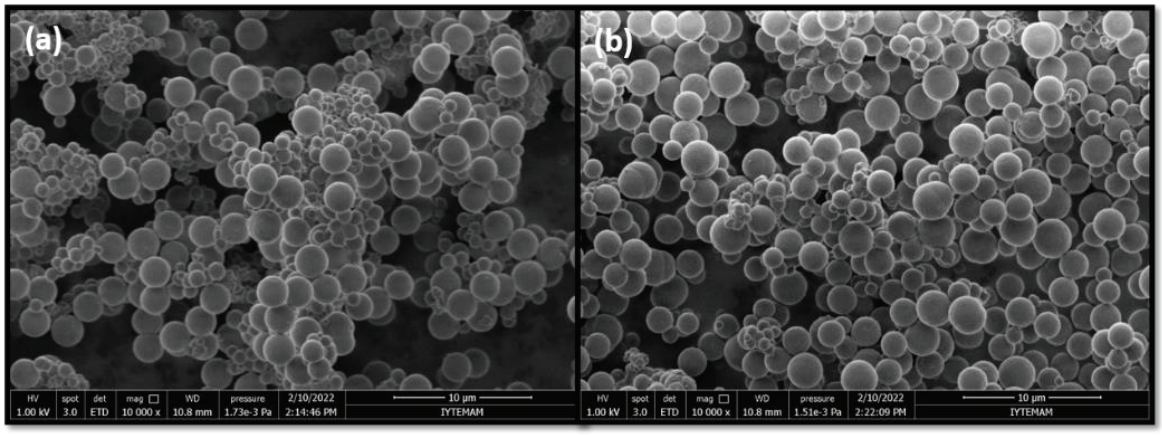

Figure 2.4. SEM images (a) MIP8 and (b) NIP8.

The spherical morphologies of MIP8 and NIP8 can be explained by the ratio of total monomer to porogen (w/v %, total monomer/porogen). This ratio is generally calculated before the synthesis for the predetermination of morphology. Smaller ratios than 5 % are expected to cause precipitation polymerization and result in spherical polymer particles with homogenous binding site distribution (Cormack and Elorza, 2004; Olcer et al., 2017). If this ratio is higher than 5%, bulk polymerization occurs and the synthesized sorbents are expected to have monolithic morphology. For bulk polymerization, it is said that the polymers need to be crushed and sieved before use in SPE process (Núñez et al., 2010). The crushing process is not desired due to the possibility of damaging the special cavities created in MIP. For our syntheses, this ratio was kept smaller than 5% and for MIP8 and NIP8 it was calculated as 1.97% before the synthesis. So the spherical MIP8 and NIP8 were obtained. The average particle size for MIP8 and NIP8 are 1.59 (±0.65) μm and 1.62 (±0.55), respectively.

The particle size of the MIP8 and NIP8 were found nearly the same from the SEM images. In general, the same surface area is expected. In Table 2.12, the BET results of MIP8 and NIP8 are given. MIP8 has higher surface area and pore volume than NIP8. This

situation may be explained by the created cavities for vitamin D3 in MIP8. The pore size is smaller for NIP8. The expectation was to have higher pore size for MIP8 due to the thought of homogeneous, individually separated creation of vitamin D3 cavities. However, these cavities may not be individually separated. The real selectivity performance and the sorption capacities of the sorbents will be controlled by binding characteristic analysis.

Table 2.12. BET results of MIP8 and NIP8.

	Surface Area	Pore Volume	Pore Size
MIP8	5.1805 m^2/g	0.012427 cm^3/g	95.9512 Å
NIP8	4.1948 m^2/g	0.008886 cm^3/g	84.7326 Å

2.3.3. Binding Characteristic Assay

The main aim of this study is to determine the amount of vitamin D3 in PBS matrix to shed light on the determination of 25OHD3 in the blood in the future studies. For samples to be studied, a pre-treatment step is required to prevent the sample matrix effect on measurements (Yin et al., 2019). Protein precipitation (PP) and saponification (SN) are generally used to separate the analytes from the sample matrix and to eliminate possible interference effects. Protein precipitation is generally used to precipitate proteins in milk, milk powder and serum. Some organic solvents may reduce the solubility of proteins in solution as well as protein precipitation. After centrifugation, the supernatant can also be used in a different method to be applied later.

Acetonitrile is the most commonly used precipitant in PP (Ogawa et al., 2017). Methanol (Meunier et al., 2015), iso-propanol (Petruzziello et al., 2017) and ethanol (Granado-Lorencio et al., 2010) are generally used for this purpose.

By considering the potential solvents for PP, methanol was chosen as sample preparation solvent since it is also the mobile phase in HPLC. The experiments were done as explained in Section 2.2.4. In the initial experiments, MIP1 and NIP1 did not show successful sorption results under the conditions applied (Figure 2.5). The negative sorption result for MIP1 at 1.0 mg/L vitamin D3 is possibly due to template bleeding (vitamin D3). More important than that is the irreproducibility (high RSD) of the results which demonstrated that these results are unreliable and must be repeated. This

observation suggest that MeOH is not a proper solvent for sorption process. The hydrogen bonding between vitamin D3 and MeOH is so strong that the expected bonding between MIP1 and vitamin D3 could not actualize. For this reason, it was decided to change the solvent and to wash out the polymer sorbent carefully to avoid the possible bleeding.

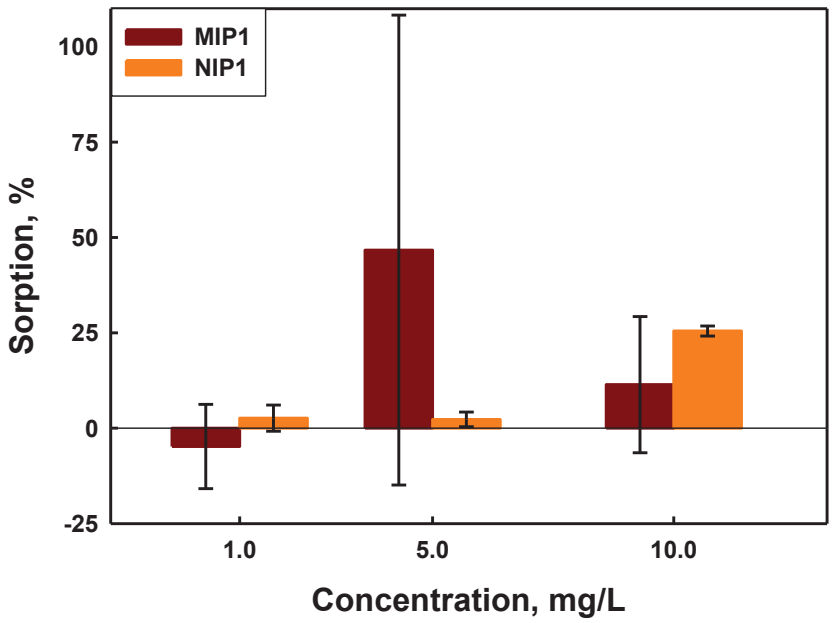

Figure 2.5. Sorption capacities of MIP1 and NIP1 using methanol as sample preparation solvent.

Secondly, acetonitrile was tried as sample preparation solvent. The experiments were done as explained in Section 2.2.4. MIP1 and NIP1 did not show a good sorption (percent sorption was less than 10%) under the conditions applied (Figure 2.6). This time bleeding did not occur due to careful washing. However, the sorption results were still low. Vitamin D3 again did not prefer to bind to the MIP1/NIP1 in acetonitrile matrix. It is clear that acetonitrile is not a proper sample matrix too.

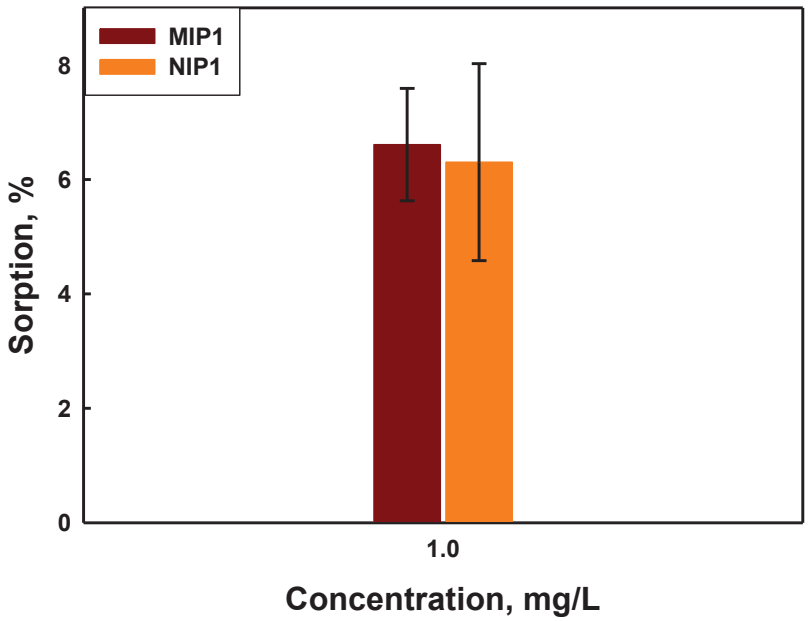

Figure 2.6. Sorption capacities of MIP1 and NIP1 using acetonitrile as sample preparation solvent.

As mentioned, vitamin D3 belongs to fat soluble vitamins group and its solubility in water is restricted. To support the hydrogen bonding between MIP1 and vitamin D3, H_2O:MeOH mixtures may be used. The logP value of vitamin D3 is 7.98, means that ratios of H_2O:MeOH between ratios of 85:15 (v/v) and 95:5 (v/v) may be used. Therefore, firstly a ratio of 90:10 (v/v) was used as mentioned in Section 2.2.4. The sorption performance was increased up to % 98 (Figure 2.7). However, as the concentration increased, the Q value suddenly decreased at 25.0 ppm and increased again at 50.0 ppm. This could be resulted from the change in solubility of vitamin D3 at these concentrations. In addition to all these, there is no difference between MIP1 and NIP1 and the high RSD of sorption results make the results unreliable to be used in an analytical measurement.

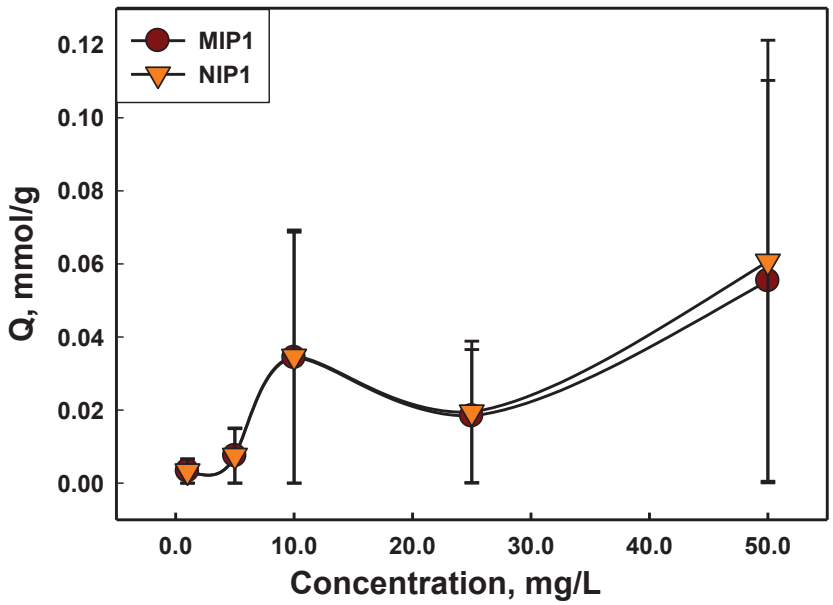

Figure 2.7. Sorption capacities of MIP1 and NIP1 using H_2O:MeOH ratio of 90:10 (v/v) mixture as sample preparation solvent at different concentrations.

Lastly, different ratios of H_2O:MeOH were tried and it was found that a ratio of 90:10 (v/v) gave the best sorption results (Figure 2.8). However, almost no difference between sorption percentages of MIP1 and NIP1 has demonstrated the need for the synthesis of new MIPs and NIPs for a better selectivity performance.

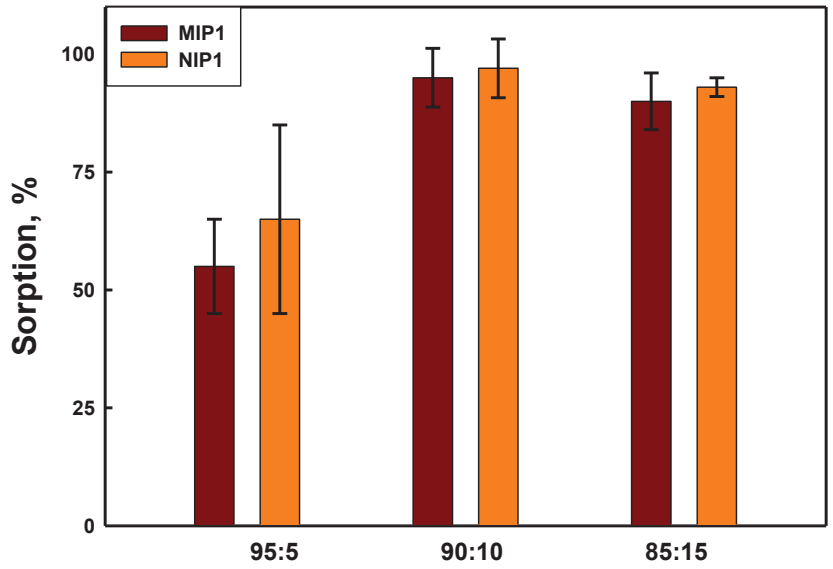

Figure 2.8. Sorption percentages of MIP1 and NIP1 at different H_2O:MeOH ratios.

The binding characteristics experiments were realized for all MIP/NIP sorbents given in Table 2.3. Among the sorbents, only MIP8/NIP8 showed significant sorption (Figure 2.9). It should be mentioned here that in order to make clear the difference between the sorption of MIP and NIP, usually high analyte concentrations are employed. For vitamin D3, high concentrations such as 50.0, 100.0, or 250.0 mg/L could not have been tried due to its limited solubility. As it is clear in Figure 22, MIP8 showed nearly 20% difference compared to NIP8 at 1.0 mg/L of 7-dehydrocholesterol (template molecule). It can be speculated that, if the trend is considered, higher differences between the sorption percentages of MIP and NIP could be expected if higher analyte concentrations were tried. Actually, the main advantage of MIP over NIP is the repeatability of the sorption (lower RSD values for all concentrations).

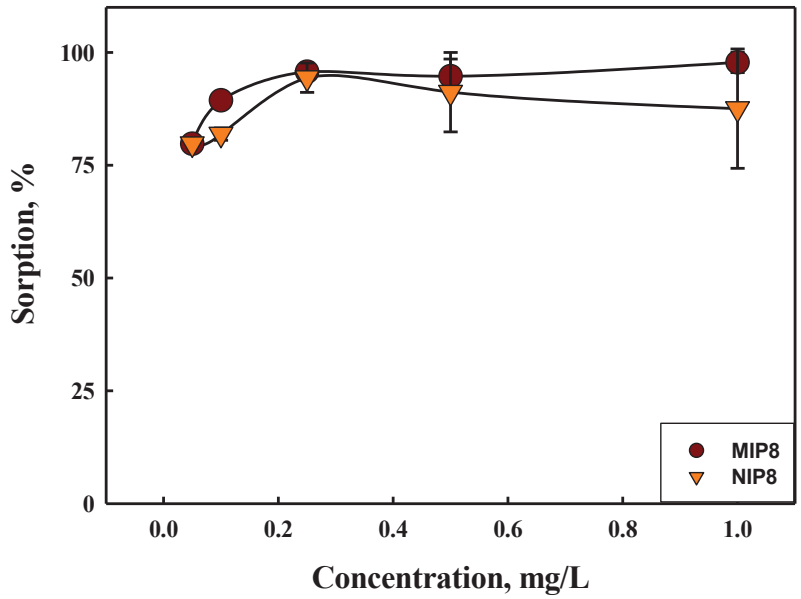

Figure 2.9. Binding characteristic assay results of MIP8 and NIP8.

Binding characteristic assay results were used for the Langmuir, Freundlich and Dubinin Radushkevich isotherm models. Figure 2.10 shows the linear fits of the three models for the sorption of 7-dehydrocholesterol by MIP8 and NIP8. The linearized forms of models were used also for the calculations of coefficients as explained in Section 1.2.1.2 and the results are summarized in Table 2.13. Based on the R^2 values, it can be said that the Freundlich and Dubinin–Radushkevich models suit better for the sorption process. For Freundlich model representing the heterogeneous surfaces, K_F (maximum absorption capacity) is ~10^6 times higher for MIP8 compared to NIP8. Dubinin–Radushkevich model, both sorption monolayer capacity (qs) and mean free energy of

sorption (E) are higher for MIP8 as expected. Langmuir model represents the homogenous monolayer coverage of sorption. It is an expected result by considering the BET results that both MIP8 and NIP8 has porous structures.

Table 2.13. Summary of Langmuir, Freundlich, and Dubinin–Radushkevich models coefficients.

Adsorption Model	Parameter	MIP8	NIP8
Langmuir	R^2	0.63	0.79
	Qmax (mmol/g)	$2.28x10^{-4}$	$5.55x10^{-4}$
	B (L/mmol)	$1.71x10^{+4}$	$7.03x10^{+3}$
Freundlich	R^2	0.88	0.82
	K_F	$5.96x10^{+7}$	$1.65x10^{+1}$
	1/n	2.48	1.08
Dubinin–Radushkevich	R^2	0.89	0.84
	B $(mol/kj)^2$	$2.00x10^{-4}$	$1.00x10^{-4}$
	qs	5.37	2.03
	E (kj/mol)	$2.00x10^{-2}$	$1.41x10^{-2}$

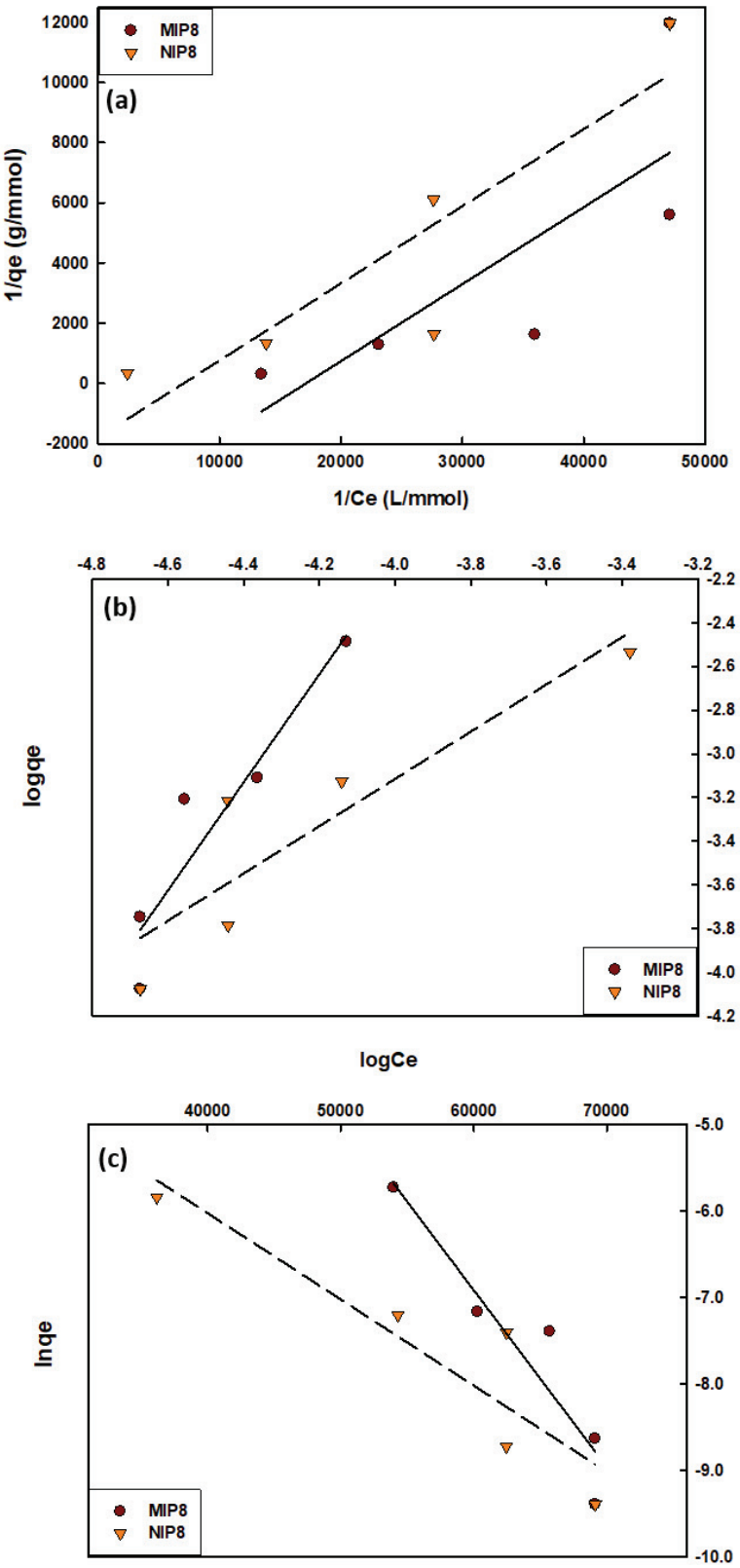

Figure 2.10. Linear fits of (a) Langmuir, (b) Freundlich, (c) Dubinin–Radushkevich models for the sorption of 7-dehydrocholesterol by MIP8 and NIP8.

2.3.4. Cross Sensitivity Experiments

Cross-sensitivity experiments were carried out to understand the sorption behavior of MIP8 and NIP8 in the presence of other structurally related compounds. Vitamin D3, vitamin D2, ergosterol, 7-dehydrocholesterol and vitamin K were added in prepared sample solution. In presence of structurally related compounds, MIP8 shows slightly better sorption (especially in terms of reproducibility) against vitamin D3 than NIP8 (Figure 2.11). 7-dehydrocholesterol behaved like dummy molecule for the detection of the vitamin D3. In other words, an MIP selective to vitamin D3 was obtained by the usage of a dummy molecule namely 7-dehydrocholesterol, the steroid form of vitamin D3.

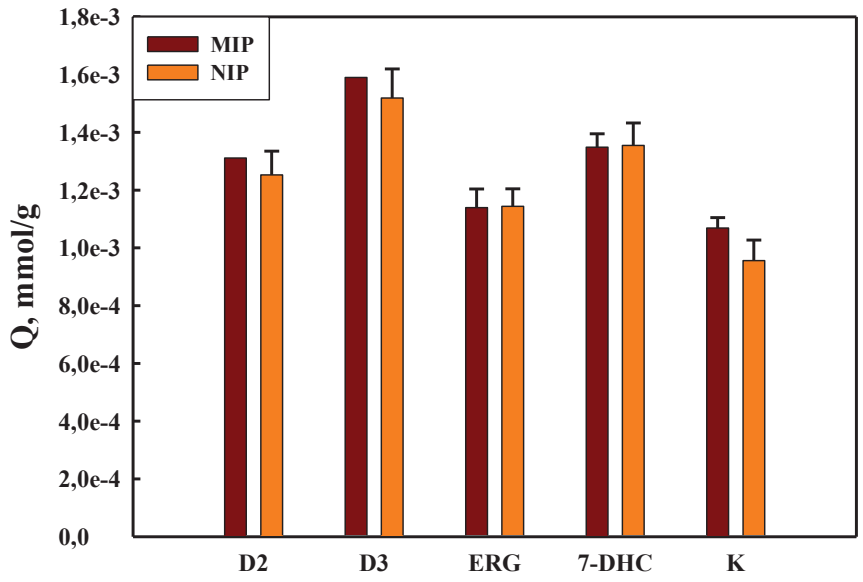

Figure 2.11. Sorption performances of MIP8 and NIP8 in the presence of other structurally related compounds.

The structures of vitamin D derivatives are similar to each other with small differences. From this point of view, 7-dehydrocholesterol, which is more economical to supply, has been used in the MIP synthesis. Cross-sensitivity experiments indicate that 7-dehydrocholesterol, which provides the synthesis of vitamin D3 in the skin, acts as a dummy molecule and the MIP synthesized with the use of 7-DHC as the template shows the highest selectivity against vitamin D3. While a difference was observed between MIP8 and NIP8 in binding experiments with 7-dehydrocholesterol, this difference

disappeared when vitamin D3 was added to the working solution, and the selectivity can be said to have shifted to the vitamin D3 molecule. In addition, NIP8 showed high bias as well as low sorption for all analytes compared to MIP. Results in Q (mmol/g) represent the value in mmol of the analytes bound to 10 mg of MIP-NIP. The reason for the low Q values is that the concentration of all analytes in the working solution is 1.0 mg/L. Since MIP8 synthesized by using 7-dehydrocholesterol as the dummy template molecule, which is the precursor of vitamin D3, showed higher sorption towards vitamin D3 compared to other compounds, it was decided to continue the method parameter optimization experiments (sorption time, amount of sorbent, etc.) with vitamin D3.

2.3.5. Effect of Sorption Time

The 24-hour sorption time used in characterization studies is quite long and impractical. Therefore, the sorption time was determined first. Figure 2.12 shows the effect of interaction time between synthesized MIP and vitamin D3 on sorption. Based on this graph, it can be said that MIP reached its maximum sorption at 5 hours. Therefore, a sorption time of 5 hours was used in the further SPE sorption studies.

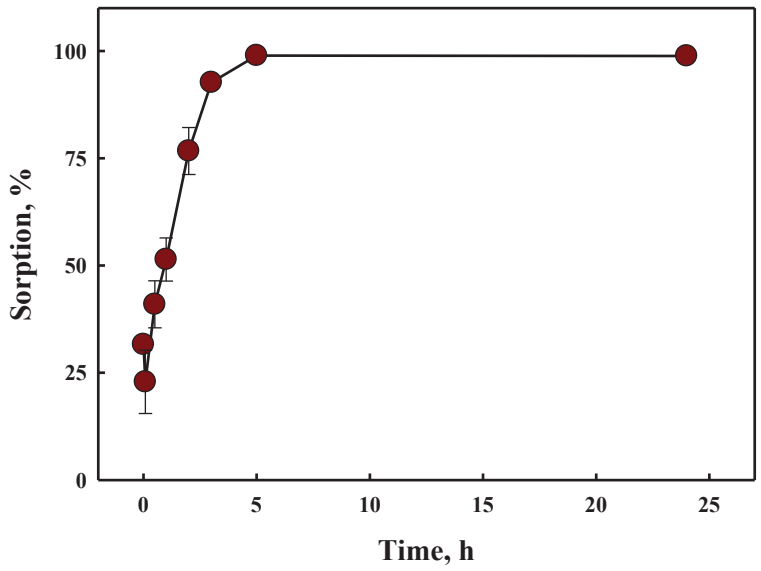

Figure 2.12. Effect of shaking time on sorption.

2.3.6. Effect of Sorbent Amount

For each amount of MIP8 sorbent given in Table 3, batch type SPE procedure was applied and the results are shown in Figure 2.13. The sorption was quantitative even at 5.0 mg and this amount was used in the remaining experiments.

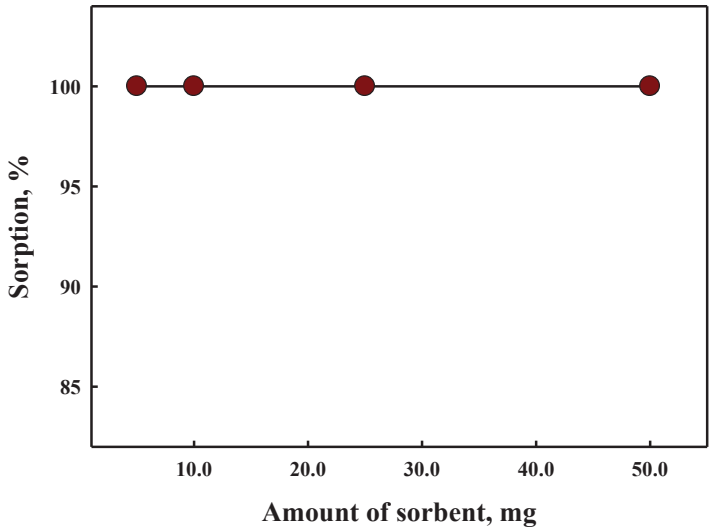

Figure 2.13. Effect of sorbent amount on sorption.

2.3.7. Effect of Sample Volume

The effect of sample volume in sorption percentage was investigated. Figure 2.14 shows that, when 5.0 mg of MIP was used with the optimized conditions, the sorption from 1.0, 5.0, 10.0 and 15.0 mL of 1.0 mg/L vitamin D3 solutions was all quantitative. Although 1.0 mL of sample volume is sufficient for analysis, 5.0 mL was chosen due to the ease of dealing with this volume.

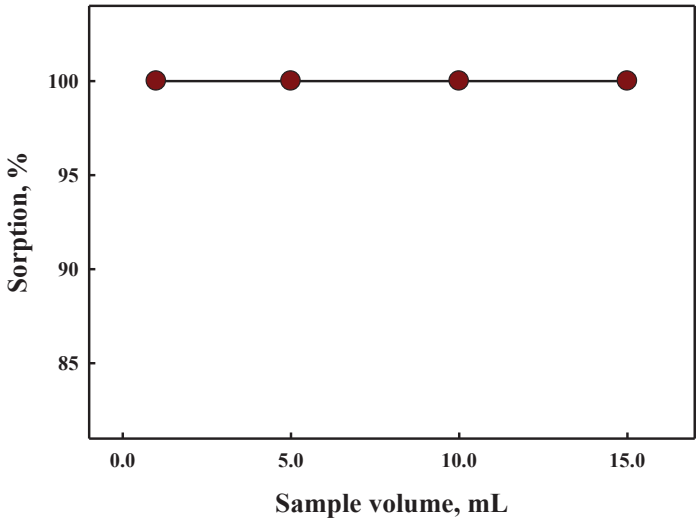

Figure 2.14. Effect of sample volume on sorption.

2.3.8. Comparison of Sorption Performance with Other Sorbents

The performance of MIP8 was compared with NIP8 and some commercial column filling materials; namely, HLB and C30. As it is clear in Figure 2.15, the sorption performance of MIP8 was slightly better than the other sorbents in terms of sorption percentage and relative standard deviation.

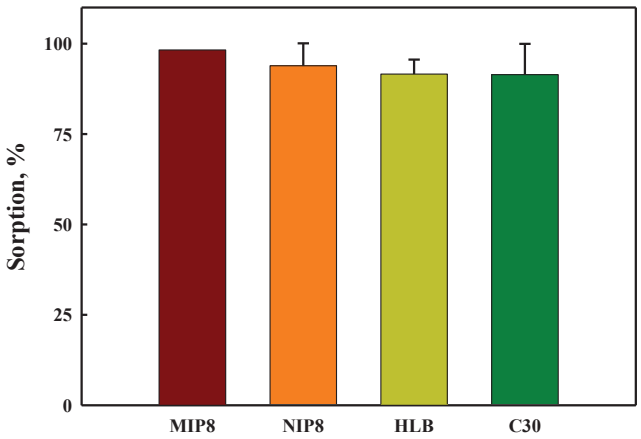

Figure 2.15. Comparison of sorption performance of MIP8 with NIP8 and commercial HLB and C18 sorbents.

2.3.9. Effect of Eluent Type

Desorption is equally important part of the SPE process as the sorption. Therefore, the analyte sorbed should ideally be recovered quantitatively from the sorbent with a proper eluent. Three different eluents were tried for desorption. Methanol (MeOH), MeOH:H_2O (90:10, v/v) and MeOH:HOAc (90:10, v/v) were tried as eluents. Figure 2.16 shows that MeOH:HOAc (90:10, v/v) gives better desorption performance (>97%) and this mixture was used in the further experiments.

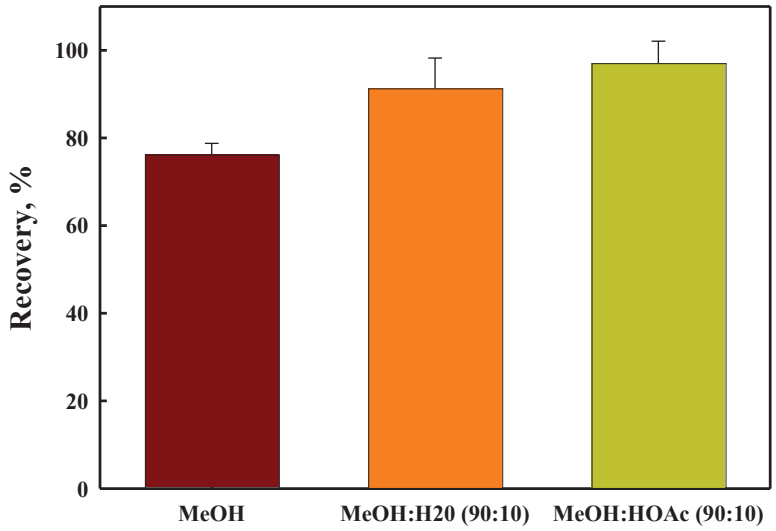

Figure 2.16. Effect of different eluents on desorption.

2.3.10. Spike Recovery Tests

The validity of proposed method was investigated in two different sample matrixes; namely H_2O:MeOH (90:10, v/v) and PBS:MeOH (90:10, v/v). Since the effluent cannot be introduced to HPLC directly, the total recovery of the method is calculated from the eluate. Spike recoveries in H_2O:MeOH (90:10, v/v) and PBS:MeOH (90:10, v/v) were calculated as 97.1 (±4.9) and 85.1 (±4.3), respectively (Figure 2.17). Although the spike recovery result of PBS:MeOH (90:10, v/v) matrix is lower than the H_2O:MeOH (90:10, v/v) matrix, repetitive analyses showed that this percentage can used

also for the exact determination of vitamin D3. The low recovery (desorption) value belongs to PBS:MeOH (90:10, v/v) solution can be related to solubility problem of vitamin D3 which effects the free concentration available for extraction.

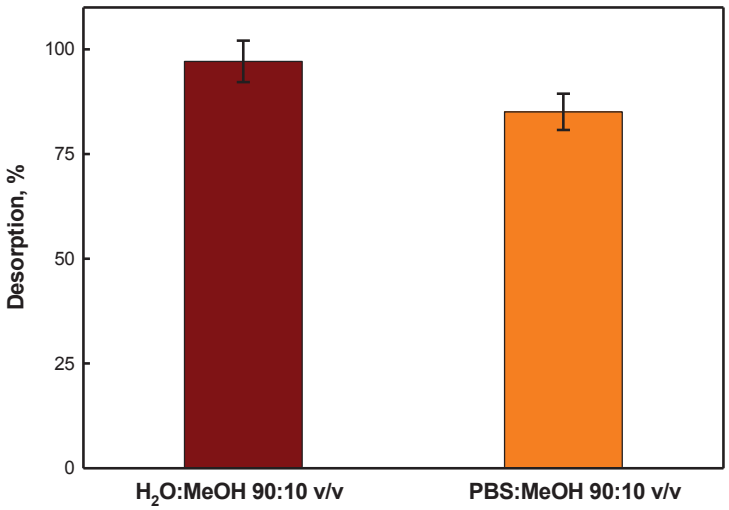

Figure 2.17. Validation of the proposed method with spiked H_2O:MeOH (90:10, v/v) and PBS:MeOH (90:10, v/v) samples.

2.3.11. Calibration Strategies

In calibration strategies, first of all the effect of SPE methodology was tested. Firstly, aqueous calibration applied by introducing different concentrations of vitamin D3 H_2O:MeOH (90:10, v/v) matrix. Then, to these solutions proposed SPE method was applied. In Figure 2.18, both aqueous calibration and matrix-matched calibration that were achieved in H_2O:MeOH (90:10, v/v) sample matrix are given. As in spiked samples in Section 2.3.10, desorption of ~97 % were obtained. Secondly, matrix-matched calibration applied to different concentrations of vitamin D3 in PBS:MeOH (90:10, v/v) matrix. From Figure 2.18, it is clear that suppression effect of sample matrix occurs. This situation also explains the decrease in desorption in Section 2.3.10.

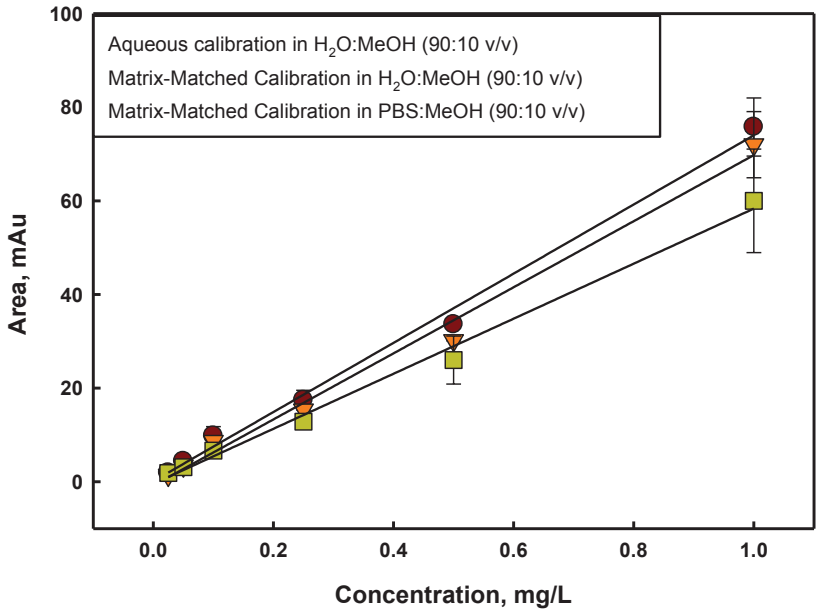

Figure 2.18. Aqueous calibration and matrix-matched calibration results.

CHAPTER 3

DETERMINATION OF VITAMIN D3 BY QUARTZ CRYSTAL MICROBALANCE

3.1. Aim of the Study

The main aim of this study is to use QCM as a scale that can detect small amounts of vitamin D3 in sample solution. Firstly, to select the most suitable surface coating, monomer and monomer mixture compositions were studied by cyclic voltammetry, for the determination of vitamin D3. Cycle number, voltage range and scan rate were investigated to find the optimum electropolymerization conditions of monomers. Then the mass-transfer ability of the selected polymer film was analyzed by using potentiostatic impedance. The eQCM was used to have thin polymer films by using optimized parameters of electropolymerization during CV analysis. Finally, the determination of vitamin D3 was achieved by QCM.

3.2. Experimental

3.2.1. Instrumentation

Electrochemical measurements were performed with Gamry Interface 1010E instrument. Gold (Au) electrode was used as the working electrode (WE) with the diameter of 2 mm. Also a Ag/AgCl was used as the reference electrode, and a Pt flake as the counter electrode (CE).

3.2.2. Thin Film Coating by Cyclic Voltammetry

Cyclic voltammetry was used to select the correct monomer or monomer compositions before coating the QCM crystal. Two monomers used in Chapter 2, namely, methacrylic acid and 4-vinylpyridine were investigated as monomers during the electropolymerization.

3.2.2.1. Modification of Working Electrode with poly(aniline-co-methacrylic acid)

The electrochemical polymerization of poly(aniline-co-methacrylic acid) was achieved on gold WE surface by cyclic voltammetry. Firstly, the WE surface was coated by using 0.1 M aniline and 0.1 M MAA mixture in 1.0 M H_2SO_4. Polymerization performed by the application of 10 potential cycles between -0.3 to 0.90 V by cyclic voltammetry at a scan rate 10 mV/s. The working voltage range was determined by using 1.0 M H_2SO_4 solution. This film was accepted as NIP film. Then, the electropoymerization was repeated by adding 7-dehydrocholesterol into the polymerization solution used during the NIP formation. Also, for comparison, 0.1 M aniline solution in 1.0 M H_2SO_4 was prepared and electropolymerized in same manner. Both MIP/NIP films were exposed to vitamin D3 solution for 5 potential cycles between -0.2 and6 -0.6V at a scan rate 10 mV/s.

3.2.2.2. Modification of Working Electrode with poly(4-vinylpyridine)

The electrochemical polymerization of poly(4-vinylpyridine) was achieved on gold WE surface by cyclic voltammetry. Firstly, the WE surface was coated by using 0.046 M 4-vinyl pyridine in 0.1 M KBr polymerization solution. Polymerization performed by the application of 10 potential cycles between -0.1 to 1.3 V by cyclic voltammetry at a scan rate 5 mV/s. The working voltage range was determined by using

0.1 M KBr solution. This film was accepted as NIP film. Then the electropoymerization was achieved by adding 7-dehydrocholesterol in a ratio of 1:12 7-dehydrocholesterol:4-VP into the polymerization solution (MIP film).

The scan rates of 50 mV/s and 30 mV/s were examined for further experiments at 10 potential cycles between -0.1 to 1.3 V. After the determination of scan rate, the MIP and NIP films were exposed to 1.0 mg/L vitamin D3 solution.3.2.3. Selectivity Control of the Prepared MIP/NIP films to Vitamin D3 by Potentiostatic Impedance

3.2.3. Selectivity Control of the Prepared MIP/NIP films to Vitamin D3 by Potentiostatic Impedance

3.2.3.1. Potentiostatic Impedance against Increasing Concentration of Vitamin D3

Selectivity of the imprinted (MIP) and non-imprinted (NIP) poly(4-vinylpyridine) films were evaluated against 0.10, 0.25, 0.50 and 1.0 mg/L vitamin D3 solution prepared in PBS:MeOH (90:10, v/v). PBS:MeOH (90:10, v/v) solution was used as blank. After introduction of each concentration MIP/NIP coated Au electrode was washed with MeOH for the removal of absorbed vitamin D3. Firstly, open circuit potentials (OC) were obtained for 10 minutes for at the vitamin D3 concentration to be analyzed. After that, EIS was applied with an AC voltage 10 mV rms for the frequencies from 100.000 Hz to 0.1 Hz for 10 points/decay. After each OC/EIS at different concentration, washing process with MeOH was applied.

3.2.3.2. Cyclic Potentiostatic Impedance Against Constant Concentration of Vitamin D3

Selectivity of the imprinted (MIP) against non-imprinted (NIP) poly(4-vinylpyridine) films were studied in 1.0 mg/L vitamin D3 solution prepared in PBS:MeOH (90:10, v/v). This time, the films were exposed to 15 repetitive OC/EIS cycles without washing with MeOH, means that vitamin D3 did not removed between cycles. Open circuit time was set to 3 hours with stability of 0.05 mV/s means that when the stability achieved, IES process will start automatically. EIS was applied with an AC voltage 10 mV rms for the frequencies from 100.000 Hz to 0.1 Hz for 10 points/decay.

3.2.4. QCM Analysis for the Determination of Vitamin D3

The optimized electropolymerization parameters of poly(4-vinylpyridine) performed by the application of 10 potential cycles between -0.1 to 1.3 V by cyclic voltammetry at a scan rate of 5 mV/s as in CV method. In this experiment, the film was coated on two sided Au coated quartz crystal instead of Au working electrode. MIP synthesis was achieved in same manner by the addition of 7-dehydrocholesterol in a ratio of 1:12 7-dehydrocholesterol:4-VP into the polymerization solution.

The performance of the NIP film was investigated in various concentrations of Vitamin D3. For this purpose, 0.0025, 0.005, 0.01, 0.25, 0.5 and 1.0 mg/L vitamin D3 solutions were prepared and analyzed. NIP film was exposed to 8.0 mL of these solutions for 5 minutes. After each concentration the film was also exposed to the 8.0 mL of MeOH for the removal of absorbed vitamin D3 for 5 minutes. The mass change on film was determined by QCM.

The performance of the NIP film was compared with bare Au coated quartz crystal. For this purpose, 0.0025, 0.005, 0.01, 0.25, 0.5 and 1.0 mg/L vitamin D3 solutions were prepared and analyzed. Both crystals were exposed to 8.0 mL of these solutions for 5 minutes. Than they were washed with 8.0 mL of MeOH for removal of vitamin D3 and the mass changes at 3th minute were controlled.

3.3. Results and Discussion

3.3.1. Thin Film Coating by Cyclic Voltammetry

3.3.1.1. Modification of Working Electrode with poly(aniline-co-methacrylic acid)

The main purpose of this part is to use the methacrylic acid as monomer in MIP/NIP synthesis for the selective determination of Vitamin D3. As mentioned before the use of a second monomer as crosslinking agent during the thin film formation decreases the selectivity due to non-selective binding sites (Munawar et al., 2020). Methacrylic acid polymerization is achieved via radical polymerization in the presence of an initiator, and the resulting poly(methyl methacrylate) (PMMA) is an insulating polymer. This feature restricts its application in electrochemisty. Consequently, the use of a second conducting polymer is needed in structure to supply conductivity (Abu Hassan Shaari et al., 2021). In modern electronic devices, the usage of conducting polymers supplies reversible doping/dedoping, controllable electrochemical properties. Polyaniline (PANI) is the most abundant conducting polymer with excellent electronic and optical properties, good redox behavior and stability (Bober, Humpolíček et al. 2015). The combination of electrical properties of PANI and the mechanical properties of PMMA found useful applications in electrochemisty (Jia et al., 2017).

Figure 3.1 shows the comparison of cyclic voltammograms of MIP, NIP and PANI. It is clear that the addition of MAA in to the polymerization solution for the formation of NIP film decreases the oxidation-reduction peaks of overall system as expected. However, the addition of template molecule, namely 7-dehydrocholesterol for the formation of MIP increases the oxidation-reduction peaks. This means that in MIP film, more functional areas for oxidation-reduction are created compared to both PANI and NIP.

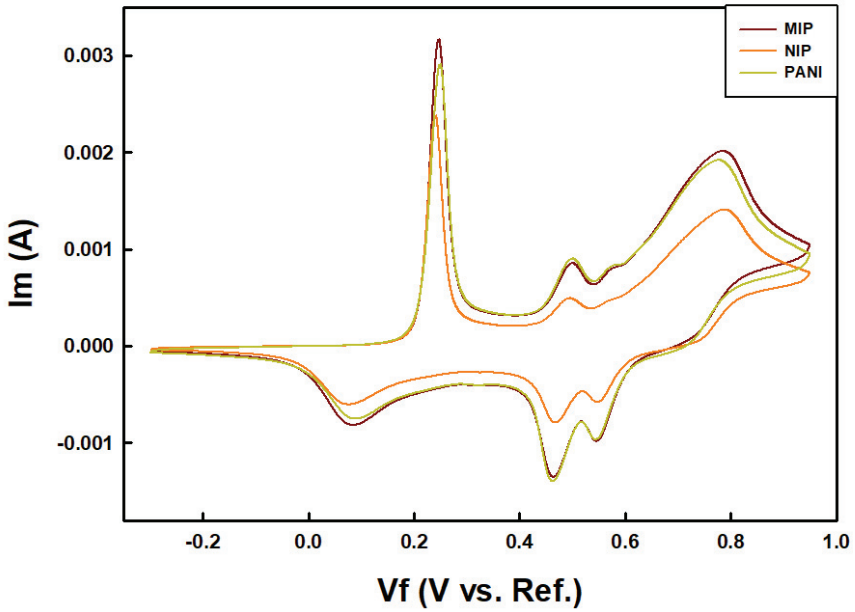

Figure 3.1. Cyclic voltammograms of MIP, NIP and PANI films.

When the film was exposed to 1.0 mg/L vitamin D3 solution in PBS:MeOH (90:10, v/v) the oxidation reduction peaks were disappeared. Figure 3.2 shows the MIP response to 1.0 M H_2SO_4 solution with oxidation reduction peaks and to 1.0 mg/L vitamin D3 solution in PBS:MeOH (90:10, v/v).

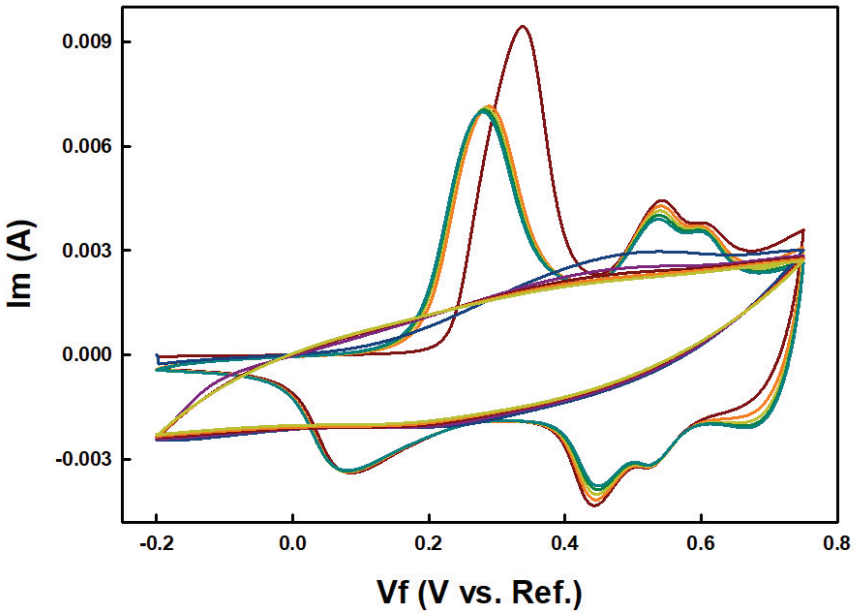

Figure 3.2. Voltammogram of MIP in exposed to1.0 M H_2SO_4 and 1.0 mg/L vitamin D3 solution in PBS:MeOH (90:10, v/v).

It is worth mentioning that during the synthesis of PANI an acid dopant is needed to improve the conductivity. The common dopants used for this purpose are hydrochloric acid (HCl) and sulphuric acid (H_2SO_4) (Banerjee et al., 2019; Bortamuly et al., 2020; Zhai et al., 2020). The redox activity of the PANI is supplied by the deprotonation of its nitrogen atom at pH < 4 (Bober et al., 2015; Song et al., 2013). At higher pH values it loses its conductivity, and the oxidation-reduction peaks disappear. In this study, PBS solution is used as solution matrix at pH 7.4. Therefore, it was expected that the addition of a second monomer, MAA, as specific binding sites can overcome this problem (Homma et al., 2012). However, this approach did not work suggesting that there is a need for a different monomer for the MIP/NIP synthesis.

3.3.1.2. Modification of Working Electrode with poly(4-vinylpyridine)

Electropolymerized poly(4-vinylpyridine) is reported in literature for the anion or cation uptake in literature (Menegazzo et al., 2012; Viel et al., 2003; Wee Ling et al., 2012). The electro-polymerization is achieved generally in supporting salts (Lebrun et al., 1996). The usage of electro-polymerized poly(4-vinylpyridine) for the detection of organic compounds in aqueous medium is also found in literature (Munawar et al., 2020).

In this part the MIP and NIP synthesis were achieved as in Section 3.2.2.2. Figure 3.3 shows the voltammogram of MIP/NIP films exposed to 0.1 M KBr.

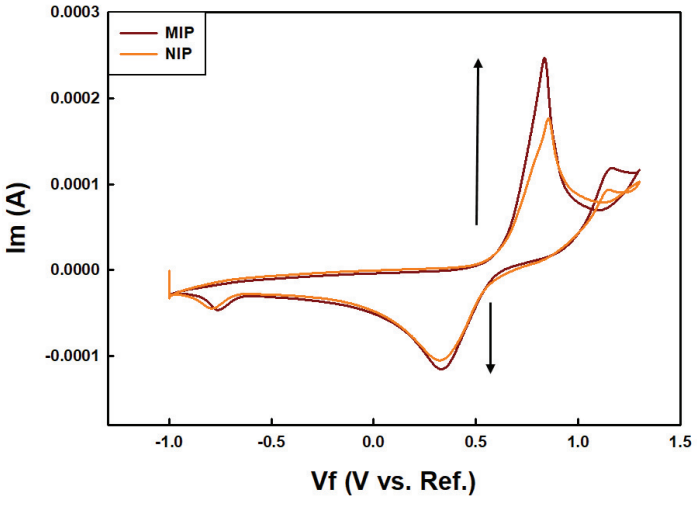

Figure 3.3. Voltammogram of MIP/NIP films exposed to 0.1 M KBr solution.

It is clear that the addition 7-dehydrocholesterol for the synthesis of MIP film increases the oxidation-reduction peaks of film. This means that more functional areas for oxidation-reduction are created in MIP compared to NIP.

The scan rate of 50 mV/s and 30 mV/s was examined. Figure 3.4 shows the voltammograms of exposing process to 0.1 M KBr by using different scan rates for both MIP (a) and NIP (b). It is 50 mV/sec scan rates give higher oxidation-reduction peaks compare to 30 mV/sec scan rate. The higher the peaks make the sorption results more distinguishable when the coating exposed to the analyte solution. So, 50 mV/sec was determined as scan rate for further experiments.

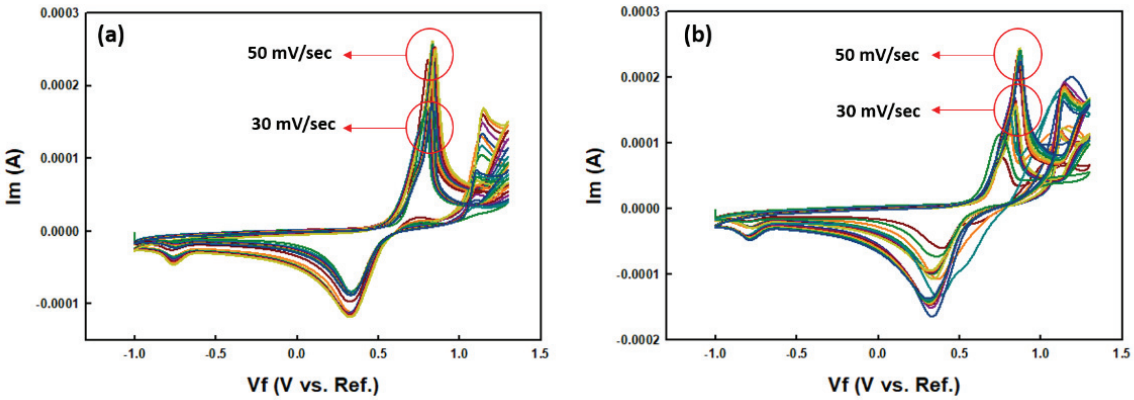

Figure 3.4. Voltammograms of exposing process to 0.1 M KBr by using different scan rates for both MIP (a) and NIP (b).

MIP and NIP coatings also exposed to the1.0 mg/L vitamin D3 solution in PBS:MeOH (90:10, v/v) (Figure 3.5). As expected MIP and NIP oxidation-reduction peaks decrease. It is thought that the vitamin D3 make hydrogen bond with MIP/NIP films. This is why the oxidation-reduction ability of films decreased by decreasing the conductivity of film (Ngwanya et al., 2021). Vitamin D3 is an electroactive compound that shows an irreversible oxidation (Lovander et al., 2018). If the oxidation of vitamin D3 occurred at this applied voltage range, there would not be a change in reduction peaks. To understand the interactions between vitamin D3 and MIP/NIP films EIS method will be used.

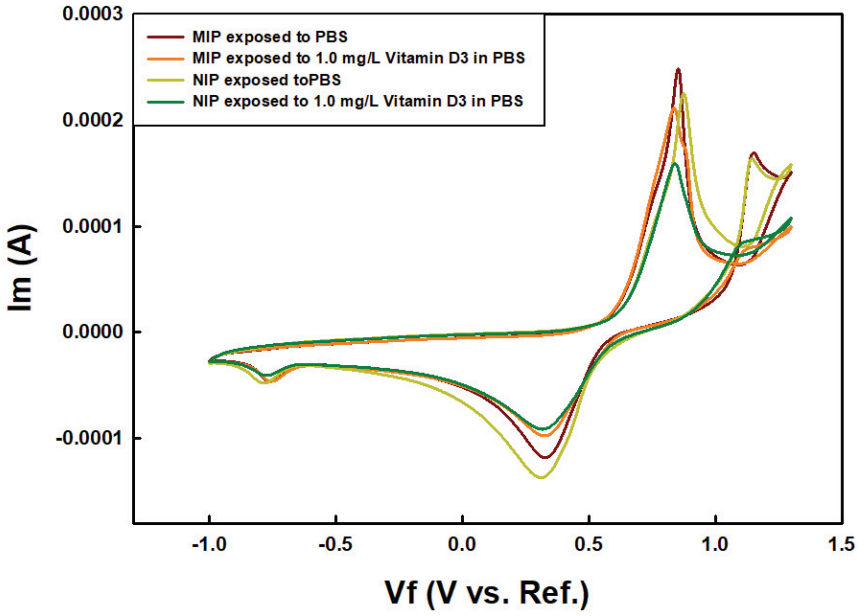

Figure 3.5. MIP and NIP coatings also exposed to the1.0 mg/L vitamin D3 solution in PBS:MeOH (90:10, v/v).

In Figure 3.6, gold electrode (a), the tip of the gold electrode (b) poly(4-vinylpyridine) MIP. MIP and NIP films have no differences in appearance, because the imprinted sites cannot be seen by this way. In literature, generally the surface of the MIP/NIP films were controlled by AFM method. However, the MIP/NIP films cannot be removed monolithically from the surface of the gold working electrode.

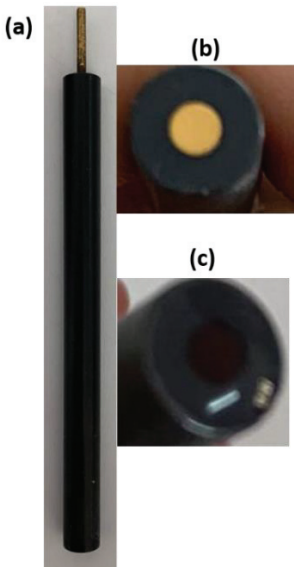

Figure 3.6. The pictures of gold electrode (a), the tip of the gold electrode (b) poly(4-vinylpyridine) MIP.

3.3.2. Selectivity Control of the Prepared MIP/NIP films to Vitamin D3 by Potentiostatic Impedance

3.3.2.1. Cyclic Potentiostatic Impedance against Increasing Concentration of Vitamin D3

The MIP/NIP films obtained by CV tested against increasing concentration of vitamin D3 in PBS:MeOH (90:10, v/v). Figure 3.7 shows the Nyquist diagrams of MIP(a) and NIP(b) at different concentrations of vitamin D3. It is clear that the concentration did not change the impedance of the system. However, it is clear that the interaction of the MIP/NIP film with vitamin D3 dependent on the mass-transfer. This mass-transfer may be time dependent and the time during the EIS process cannot be sufficient for this mass transfer. To clarify this problem, MIP/NIP films are exposed to the 1.0 mg/L vitamin D3 solution for successive cycles without desorbing the films with MeOH.

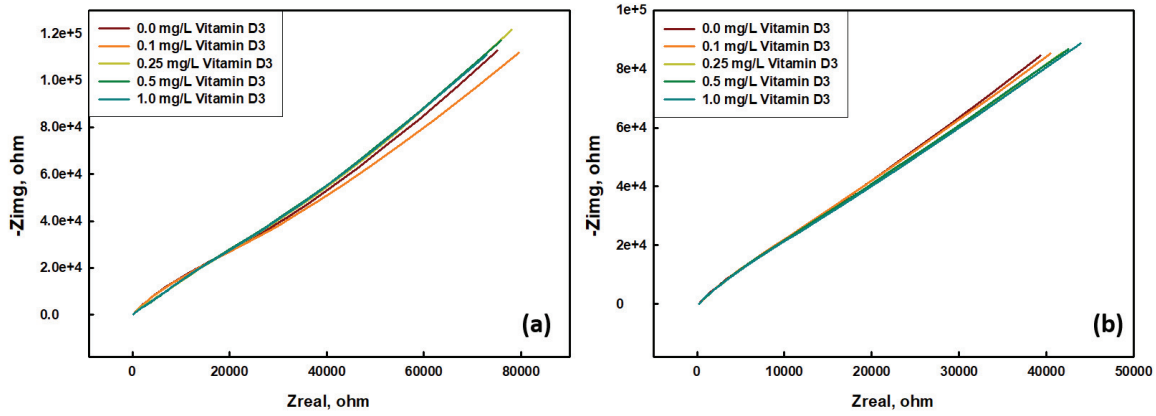

Figure 3.7. Nyquist diagrams of MIP(a) and NIP(b) at different concentrations of vitamin D3.

3.3.2.2. Cyclic Potentiostatic Impedance Against Constant Concentration of Vitamin D3

By using both MIP and NIP films obtained by CV, 1.0 mg/L vitamin D3 solution in PBS:MeOH (90:10, v/v) was used for potentiostatic EIS measurements. The main aim was to understand the interactions between vitamin D3 and MIP/NIP films by using EIS method. The resistance of the system should increase as the vitamin D3 fills the pores of the coating. A cyclic potentiostatic impedance program was prepared. The coating was exposed to the successive open circuit potential and potentiostatic impedance cycle.

Firstly, the open circuit results were examined. During this part of the cycle, the film let to show its characteristic potential without applying voltage or current. The longer the time until the voltage stabilizes, the greater the interaction at the surface, means that higher the surface area. Also the voltage changes in successive cycles, gives information about the deposition of analyte in that coating. Figure 3.8 shows the comparison of time passed for the films for a constant voltage (a) and the final voltages during the cycles (b). As the cycle number increases the time passed for the stabilization of coating voltage is higher for MIP. This is due to the higher surface area of MIP which is caused by pores created during coating. Also voltage changes are more remarkable for MIP, because more mass diffusion occurs due to high surface area and the deposition of analyte in to the pores decreases the conductivity of film so the surface voltage decreases.

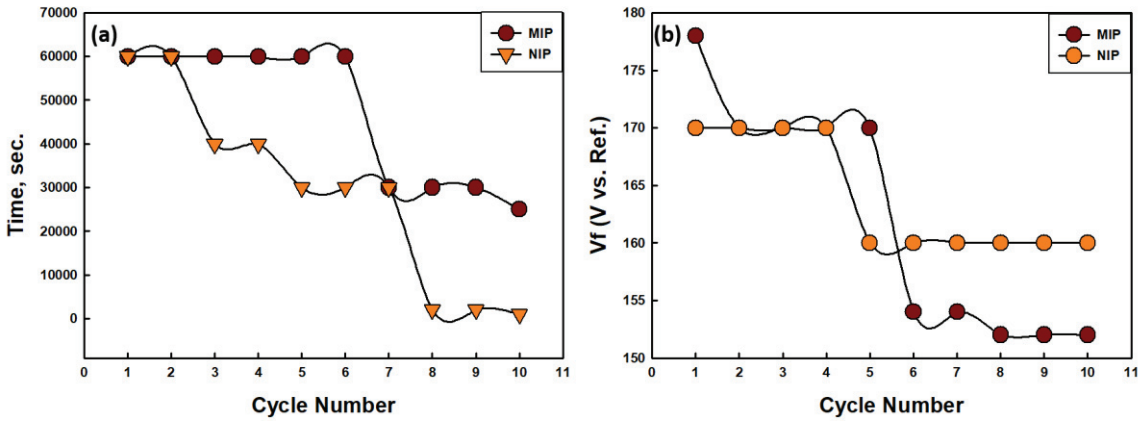

Figure 3.8. Open Circuit Potential results of successive cycles.

The Nyquist diagrams of both MIP and NIP are given in Figure 3.9. For first 10 cycles both diagrams show increase (Figure 3.9a and 3.9b). This increase explains that

the sorption occurs for both coatings. MIP shows regular increase on the contrary of NIP. It can be said that MIP shows reliable sorption capacity than NIP. After 10 cycles, MIP showed a decrease. This can be the proof of second sorption sites. If it is excepted that the sorption up to 10. cycle occurred at cavities, in these cycles (after 10) sorption occurs at the surface of the film (Figure 3.9c). For NIP, the diagram does not show any decrease (Figure 3.9d) It can be said that the highest capacity of the film has reached.

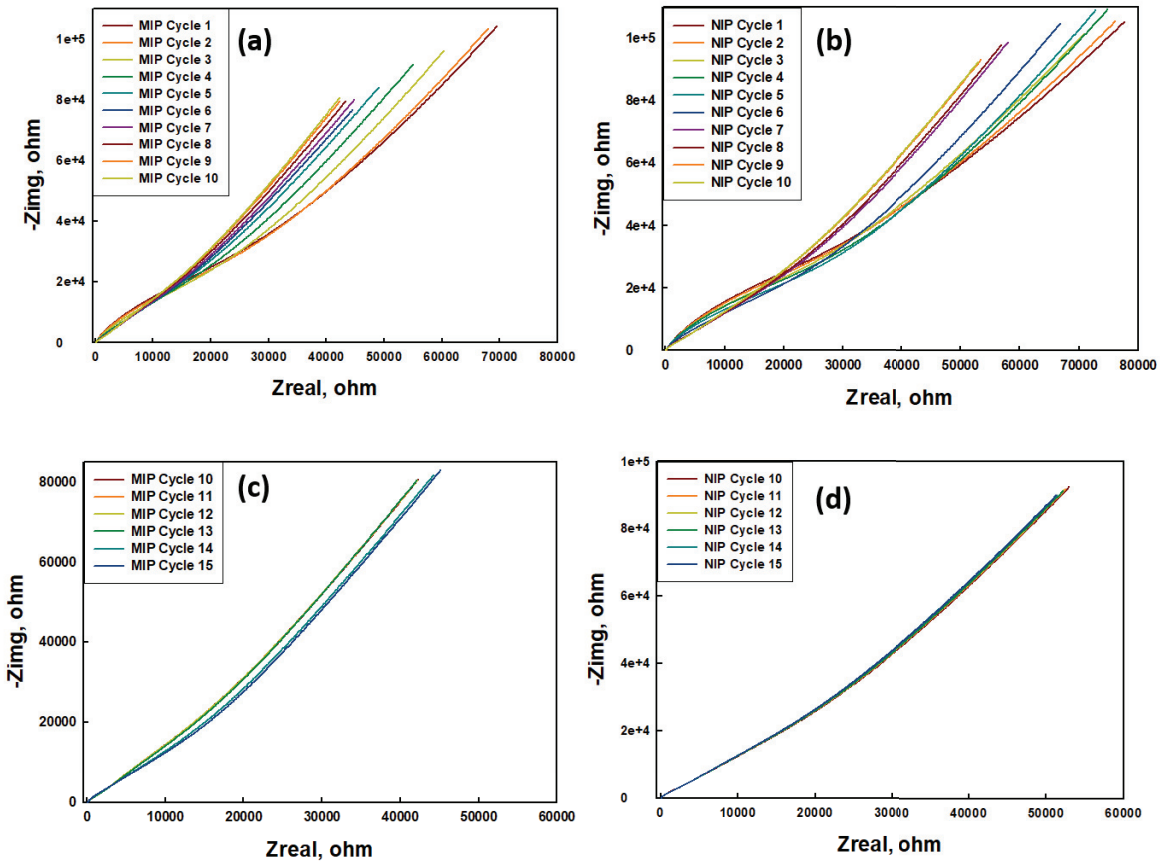

Figure 3.9. The Nyquist diagrams of both MIP and NIP.

Also to understand the warburg characteristics of the MIP and NIP, cycle 1, cycle 6 and cycle 10 were compared (Figure 3.10). At each cases MIP shows higher W than NIP, means that MIP absorbed more vitamin D3 compare to NIP. The difference reached the highest at 6. cycle and it can be correlate with the results of open circuit potential results (Figure 3.8b) that MIP showed a sudden decrease.

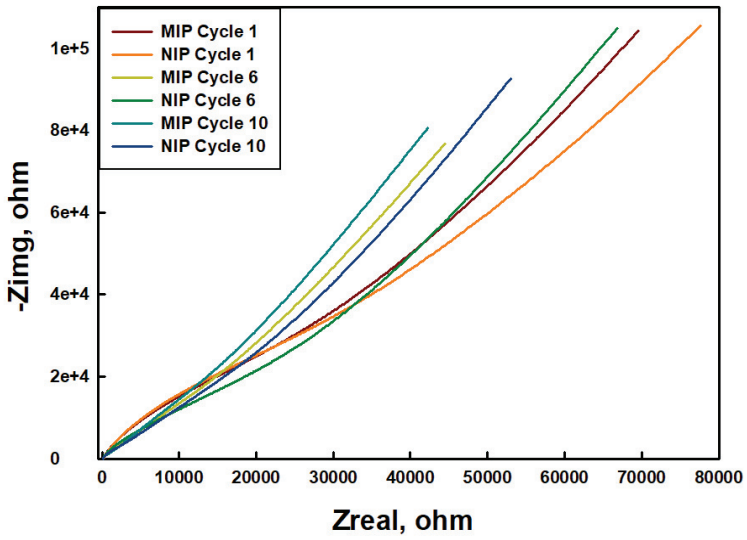

Figure 3.10. Comparison of cycle 1, 6 and 10 Nyquist Diagrams of MIP and NIP.

In Figure 3.11, capacitance of electrical double layer, C_{dl} (a) and Warburg impedance, W (b) change of successive cycles are given. Due to the porous structure of MIP, it accepts ions higher than NIP at the beginning, showing higher C_{dl}. However, decrease in C_{dl} occurs due to mass-transfer at the same time. Mass transfer blocks the charge transfer. In NIP case, C_{dl} suddenly decrease due to low mass-transfer ability of the film and became constant. As a result, the rapid decrease of C_{dl} value of NIP occurs rapidly due to low sorption capacity, that is, low mass transfer ability, while it occurs slowly in MIP due to high mass transfer ability. In W, a rapid increase is observed in MIP due to its mass transfer ability.

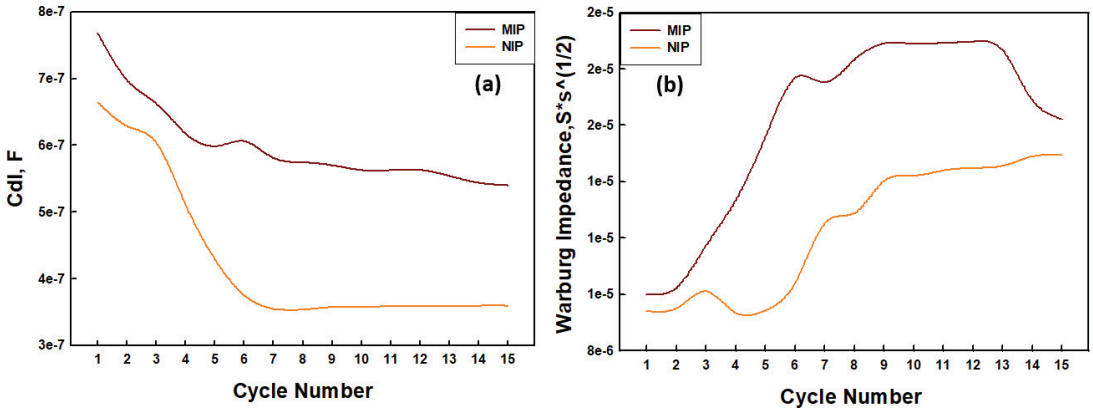

Figure 3.11. Capacitance of electrical double layer, Cdl (a) and Warburg impedance, W (b) change of successive cycles.

3.3.3. QCM Analysis for the Determination of Vitamin D3

QCM probes were produced by electrodeposition of poly-4-vinylpyridine under the identical conditions. The loading mass of the optimal NIP film on the QCM probe was estimated from Sauerbrey Equation to be 500 micrograms, and the estimated thickness to be about 200 nm. The obtained optimum QCM probe was place in the electrochemical cell for the frequency measurement in air. Analyte solutions were carefully added to the cell while the frequency of measurement to avoid the data loss for 5 minutes. Obviously, the corresponding mass of the QCM probe increased quickly in a denser environment, then decreased for all solutions. Having reach an equilibrium, the QCM probe began to extract the analyte at a certain point in each solution. As can be seen in Figure 3.12, the extraction of the QCM probe was increased in high solutions, indicating strong binding of vitamin D3 in a short time. However, the QCM probe mass did not almost change in 2.5 ppb solution while it is showing a good performance in 10 ppb analyte solution. The detection limit of the QCM probes was related to the chemical and physical properties that the thicker film can be a convenient solution to decrease the detection limit. The detection limit of QCM probes was related to chemical and physical properties where thicker film could be a viable solution to reduce detection limit.

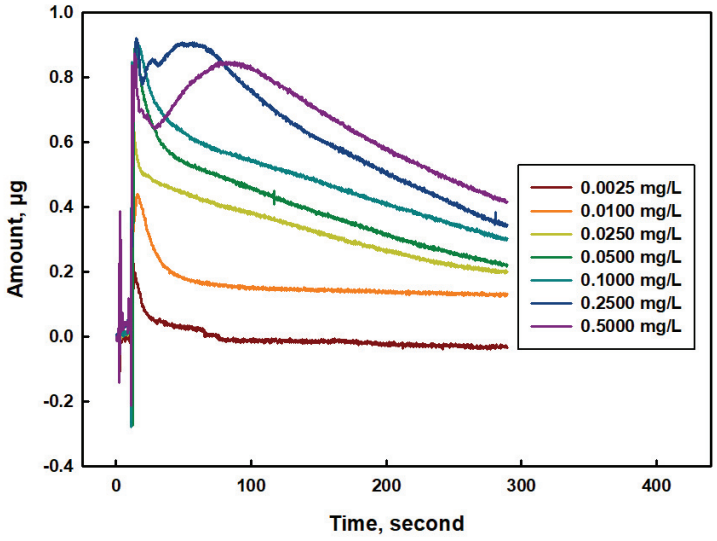

Figure 3.12. The extraction of the QCM probe with increased concentration of vitamin D3.

In Figure 3.13, the mass changes occurred at increasing concentration of vitamin D3 for poly(4-vinylpyridine) coated crystal (NIP) and bare Au coated quartz crystal at 3th minute are given. It is clear that as the concentration increases the amount of vitamin D3 absorbed on NIP film coated quartz increasing. However, for bare gold quartz crystal, the absorbed vitamin D3 amount against increasing concentration did not show a regular increase. It can be said that poly(4-vinylpyridine) coated crystal shows more reliable results compare to bare Au coated quartz crystal. The results obtained by poly(4-vinylpyridine) coated crystal for the quantification of vitamin D3 in aqueous samples may keep a light to further experiments.

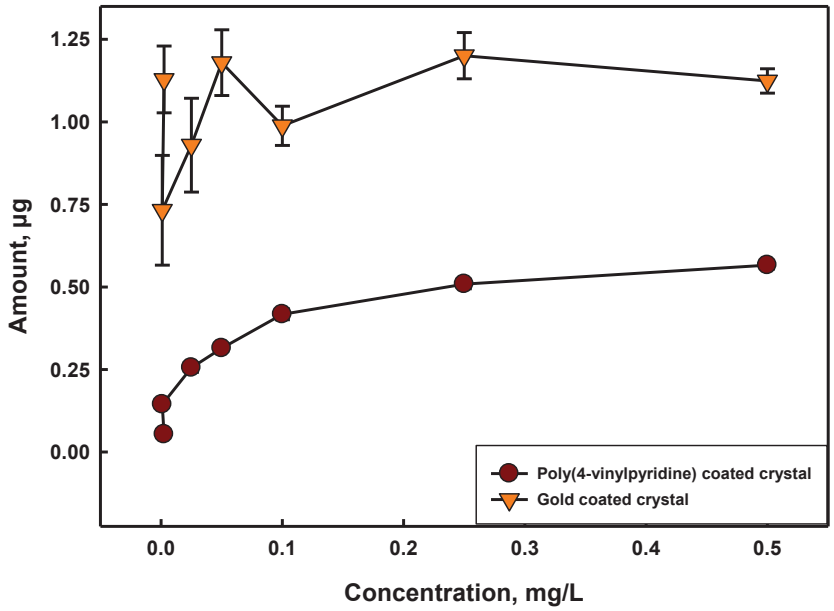

Figure 3.13. The extraction performance of the poly(4-vinylpyridine) coated crystal and gold coated crystal with increased concentration of vitamin D3.

CHAPTER 4

CONCLUSION

In this study, basically two different polymerization techniques were used to obtain MIP/NIP sorbents/films for the detection of vitamin D3. Firstly, MIP/NIP sorbents were synthesized by precipitation polymerization for proposing SPE method prior to HPLC-DAD analysis. Experimental parameters were determined as follows; sorbent amount of 5.0 mg for 5.0 mL of 1.0 mg/L vitamin D3 in 90:10 (v/v) ratio of H_2O:MeOH solution with a sorption time of 5 hours and MeOH:HOAc ratio of 90:10 (v/v) as desorption solution. The spike recovery test results showed that the overall recovery of the proposed method for 1.0 mg/L vitamin D PBS:MeOH in a ratio of 90:10 (v/v) was found as 85.1 % (±4.3, n=3). With the help of this SPE method, the difficulties of working with one of the lipid soluble vitamins, namely vitamin D3 tried to clarify. The solubility of vitamin D3 is the most important problem. Molecular imprinted technology depends on the attractions between the reactive site of MIP and analyte in interest by choosing the proper solvent that dissolves the vitamin D3, it is provided that the vitamin D3 remains in the cavities in the polymer instead of the solution. In case of vitamin D3, the solubility is achieved by organic solvents. However, this time sorption process did not occur. To overcome this problem, logP value was taken into the consideration and it was found that 90:10 (v/v) ratio of H_2O:MeOH is the best working solution. As the amount of vitamin D3 increases in the solution, the binding characteristic assay results showed that the solubility decreases. So during the determination of the experimental parameters, the concentration of the vitamin D3 was kept $\leq$ 1.0 mg/L.

In second part, electropolymerization of poly(aniline-co-methacrylic acid) and poly(4-vinylpyridine) achieved by CV method. It was found that the poly(aniline-co-methacrylic acid) film is not a good choice to work with working solutions prepared in PBS:MeOH (90:10, v/v). PBS solution has a pH value of 7.4. However, the redox activity of the PANI is supplied by the deprotonation of its nitrogen atom at pH < 4. The addition of a second polymer namely methacrylic acid did not change this situation and poly(aniline-co-methacrylic acid) did not give any oxidation-reduction peak for vitamin D3 solution prepared in PBS:MeOH (90:10, v/v). After that poly(4-vinylpyridine)

MIP/NIP films were electropolymerized on gold working electrode by cyclic voltammetry with the optimized parameters of 10 cycle number, -1.0 to 1.3 V voltage range and 5 mV/s scan rate. The MIP and NIP films redox properties were controlled for 5 cycle number, -1.0 to 1.3 V voltage range 50 mV/sec scan rates and found that the oxidation-reduction peak of MIP film is higher than the NIP film. This means that more active sites for oxidation-reduction and also for the recognition of vitamin D3 were created. The affinity of films to vitamin D3 were also controlled by exposing them to 1.0 mg/L vitamin D3 solution prepared in 90:10 (v/v) ratio of PBS:MeOH. The oxidation reduction peaks of the films were decreased by the vitamin D3 sorption. This means that vitamin D3 was sorbed on films irreversibly and the redox properties of the films were decreased. The sorption abilities of the films probably depend on the mass-transfer. This ability of films was controlled by analyzing the films by EIS in two ways; increasing concentration of vitamin D3 and constant concentration of vitamin D3. During the increased concentration, the films were washed with MeOH to remove the sorbed vitamin D3 species. It was observed that the interaction of poly(4-vinylpyridine) MIP/NIP films with the vitamin D3 mainly depend on the mass-transfer, not charge transfer, means that Warburg impedance dominates. The vitamin D3 concentration change in PBS:MeOH (90:10, v/v) solution was not observed during the OC and EIS analysis due to the time dependence of mass transfer process. Constant concentration trials carried out without washing the film. After the successive 16 OC/EIS cycles, it was found that the OC potential of MIP is higher than NIP at the beginning but by increasing the cycle number reversed behavior was observed. The higher the OC potential belongs to MIP is the result of higher conductivity of film compare to NIP, meaning that more oxidation-reduction areas and more areas for vitamin D3 sorption. The OC value of both MIP and NIP decreased after successive cycles and became constant after 8. cycle for MIP and 5. cycle for NIP. Higher surface area and higher sorption areas for vitamin D3 in MIP can also explain this situation. By using Randles equivalent circuit model, the Warburg impedance which represents the mass-transfer was found higher for MIP compare to NIP. The optimized electropolymerization parameters during the CV method was used in the electropolymerization of poly(4-vinylpyridine) NIP film on quartz crystal by eQCM method and the film was analyzed by QCM method. It was found that the amount of vitamin D3 as small as 0.0100 mg/L can be detected by the usage of this microscale.

REFERENCES

Abu Hassan Shaari, H., Ramli, M. M., Mohtar, M. N., Abdul Rahman, N., & Ahmad, A. (2021). Synthesis and Conductivity Studies of Poly(Methyl Methacrylate) (PMMA) by Co-Polymerization and Blending with Polyaniline (PANi). *Polymers*, *13*(12), 1939. https://www.mdpi.com/2073-4360/13/12/1939

Adsorption. (2022). Retrieved 15.05.2022 from https://en.wikipedia.org/wiki/Adsorption

Altinbas, A., Tas, N., Cebeci, Z., Cihan, M., Canakci, E., & Noyan, T. (2019). The effect of vitamin d levels on the mood disorders of the operating room and intensive care unit staff [Article]. *Journal of Clinical and Analytical Medicine*, *10*(2), 156-165. https://doi.org/10.4328/jcam.6076

Apodaca, D., Pernites, R., Ponnapati, R., Mundo, F., & Advincula, R. (2011). Electropolymerized Molecularly Imprinted Polymer Film: EIS Sensing of Bisphenol A. *Macromolecules*, *44*. https://doi.org/10.1021/ma2010525

Bahadır, E. B., & Sezgintürk, M. K. (2016). A review on impedimetric biosensors. *Artif Cells Nanomed Biotechnol*, *44*(1), 248-262. https://doi.org/10.3109/21691401.2014.942456

Baker, C. K., Qiu, Y. J., & Reynolds, J. R. (1991). Electrochemically-induced charge and mass transport in polypyrrole/poly(styrene sulfonate) molecular composites. *The Journal of Physical Chemistry*, *95*(11), 4446-4452. https://doi.org/10.1021/j100164a053

Banerjee, J., Dutta, K., Kader, M. A., & Nayak, S. K. (2019). An overview on the recent developments in polyaniline-based supercapacitors. *Polymers for Advanced Technologies*, *30*(8), 1902-1921. https://doi.org/https://doi.org/10.1002/pat.4624

Basics of Electrochemical Impedance Spectroscopy. (2022). Gamry Retrieved 06.06.2022 from https://www.gamry.com/application-notes/EIS/basics-of-electrochemical-impedance-spectroscopy/

Bendik, I., Friedel, A., Roos, F. F., Weber, P., & Eggersdorfer, M. (2014). Vitamin D: a critical and essential micronutrient for human health [Review]. *Frontiers in Physiology*, *5*(248). https://doi.org/10.3389/fphys.2014.00248

Bober, P., Humpolíček, P., Pacherník, J., Stejskal, J., & Lindfors, T. (2015). Conducting polyaniline based cell culture substrate for embryonic stem cells and embryoid bodies [10.1039/C5RA07504A]. *Rsc Advances*, *5*(62), 50328-50335. https://doi.org/10.1039/C5RA07504A

Bodnar, L. M., Simhan, H. N., Powers, R. W., Frank, M. P., Cooperstein, E., & Roberts, J. M. (2007). High prevalence of vitamin D insufficiency in black and white pregnant women residing in the northern United States and their neonates [Article]. *Journal of Nutrition*, *137*(2), 447-452. <Go to ISI>://WOS:000243779600026

Bohannan, E. W., Huang, L.-Y., Miller, F. S., Shumsky, M. G., & Switzer, J. A. (1999). In Situ Electrochemical Quartz Crystal Microbalance Study of Potential Oscillations during the Electrodeposition of Cu/Cu2O Layered Nanostructures. *Langmuir*, *15*(3), 813-818. https://doi.org/10.1021/la980825a

Bortamuly, R., Konwar, G., Boruah, P. K., Das, M. R., Mahanta, D., & Saikia, P. (2020). CeO2-PANI-HCl and CeO2-PANI-PTSA composites: synthesis, characterization, and utilization as supercapacitor electrode materials. *Ionics*, *26*(11), 5747-5756. https://doi.org/10.1007/s11581-020-03690-7

Boyaci, E., Eroğlu, A. E., & Shahwan, T. (2010). Sorption of As(V) from waters using chitosan and chitosan-immobilized sodium silicate prior to atomic spectrometric determination. *Talanta*, *80*(3), 1452-1460. https://doi.org/10.1016/j.talanta.2009.09.053

Bruckenstein, S., & Shay, M. (1985). An in situ weighing study of the mechanism for the formation of the adsorbed oxygen monolayer at a gold electrode. *Journal of Electroanalytical Chemistry and Interfacial Electrochemistry*, *188*(1), 131-136. https://doi.org/https://doi.org/10.1016/S0022-0728(85)80057-7

Chung, S.-M., Paik, W.-k., & Yeo, I.-H. (1997). A study on the initial growth of polypyrrole on a gold electrode by electrochemical quartz crystal microbalance. *Synthetic Metals*, *84*(1), 155-156. https://doi.org/https://doi.org/10.1016/S0379-6779(97)80690-X

Cormack, P. A., & Elorza, A. Z. (2004). Molecularly imprinted polymers: synthesis and characterisation. *J Chromatogr B Analyt Technol Biomed Life Sci*, *804*(1), 173-182. https://doi.org/10.1016/j.jchromb.2004.02.013

Electroanalytical methods. (2022, 28.02.2022). Wikipedia. Retrieved 18.05.2022 from https://en.wikipedia.org/wiki/Electroanalytical_methods

Fontanals, N., Marcé, R., & Borrull, F. (2010). Overview of the novel sorbents available in solid-phase extraction to improve the capacity and selectivity of analytical determinations. *Contrib. Sci.*, *6*, 199-213.

Granado-Lorencio, F., Herrero-Barbudo, C., Blanco-Navarro, I., & Pérez-Sacristán, B. (2010). Suitability of ultra-high performance liquid chromatography for the determination of fat-soluble nutritional status (vitamins A, E, D, and individual carotenoids). *Anal Bioanal Chem*, *397*(3), 1389-1393. https://doi.org/10.1007/s00216-010-3655-2

Hashim, S., Schwarz, L. J., Danylec, B., Mitri, K., Yang, Y. Z., Boysen, R. I., & Hearn, M. T. W. (2016). Recovery of ergosterol from the medicinal mushroom, Ganoderma tsugae var. Janniae, with a molecularly imprinted polymer derived from a cleavable monomer-template composite [Article]. *Journal of Chromatography A*, *1468*, 1-9. https://doi.org/10.1016/j.chroma.2016.09.004

Homma, T., Kondo, M., Kuwahara, T., & Shimomura, M. (2012). Electrochemical polymerization of aniline in the presence of poly(acrylic acid) and characterization of the resulting films. *Polymer*, *53*(1), 223-228. https://doi.org/https://doi.org/10.1016/j.polymer.2011.11.038

Hoogvliet, J. C., & van Bennekom, W. P. (2001). Gold thin-film electrodes: an EQCM study of the influence of chromium and titanium adhesion layers on the response. *Electrochimica Acta*, *47*(4), 599-611. https://doi.org/https://doi.org/10.1016/S0013-4686(01)00793-9

Jäpelt, R., & Jakobsen, J. (2013). Vitamin D in plants: a review of occurrence, analysis, and biosynthesis [Review]. *Frontiers in Plant Science*, *4*(136). https://doi.org/10.3389/fpls.2013.00136

Jia, M.-Y., Zhang, Z.-M., Yu, L.-M., & Wang, J. (2017). PANI-PMMA as cathodic electrode material and its application in cathodic polarization antifouling. *Electrochemistry Communications*, *84*, 57-60. https://doi.org/https://doi.org/10.1016/j.elecom.2017.09.021

Kasalová, E., Aufartová, J., Krčmová, L. K., Solichová, D., & Solich, P. (2015). Recent trends in the analysis of vitamin D and its metabolites in milk – A review. *Food Chemistry*, *171*, 177-190. https://doi.org/https://doi.org/10.1016/j.foodchem.2014.08.102

Kawaguchi, T., Yasuda, H., Shimazu, K., & Porter, M. D. (2000). Electrochemical Quartz Crystal Microbalance Investigation of the Reductive Desorption of Self-

Assembled Monolayers of Alkanethiols and Mercaptoalkanoic Acids on Au. *Langmuir*, *16*(25), 9830-9840. https://doi.org/10.1021/la000756b

Khadro, B., Sanglar, C., Bonhomme, A., Errachid, A., & Jaffrezic-Renault, N. (2010). Molecularly imprinted polymers (MIP) based electrochemical sensor for detection of urea and creatinine. *Procedia Engineering*, *5*, 371-374. https://doi.org/https://doi.org/10.1016/j.proeng.2010.09.125

Knox, S., Harris, J., Calton, L., & Wallace, M. A. (2009). A simple automated solid-phase extraction procedure for measurement of 25-hydroxyvitamin D3 and D2 by liquid chromatography-tandem mass spectrometry. *Annals of Clinical Biochemistry*, *46 Pt 3*, 226-230. https://doi.org/10.1258/acb.2009.008206

Komiyama, M., Takeuchi, T., Mukawa, T., & Asanuma, H. (2003). *Molecular Imprinting: From Fundamentals to Applications*.

Kumar Singh, A., & Singh, M. (2015). QCM sensing of melphalan via electropolymerized molecularly imprinted polythiophene films. *Biosens Bioelectron*, *74*, 711-717. https://doi.org/10.1016/j.bios.2015.07.027

Kushwaha, A., Srivastava, J., & Singh, M. (2022). EQCM sensor for targeting psychoactive drug via rationally designed molecularly imprinted polymeric nanoparticles (nanoMIPs). *Materials Today: Proceedings*, *49*, 3345-3356. https://doi.org/https://doi.org/10.1016/j.matpr.2021.01.344

Lebrun, C., Deniau, G., Tanguy, J., & Lécayon, G. (1996, January 01, 1996). Study of the ability of 4-vinylpyridine to form electropolymerized coatings on nickel cathodes. The proceedings of the 53rd International meeting of Physical chemistry: Organic coatings,

Leuaa, P., Priyadarshani, D., Choudhury, D., Maurya, R., & Neergat, M. (2020). Resolving charge-transfer and mass-transfer processes of VO2+/VO2+ redox species across the electrode/electrolyte interface using electrochemical impedance spectroscopy for vanadium redox flow battery [10.1039/D0RA05224H]. *Rsc Advances*, *10*(51), 30887-30895. https://doi.org/10.1039/D0RA05224H

Levi, M. D., Salitra, G., Levy, N., Aurbach, D., & Maier, J. (2009). Application of a quartz-crystal microbalance to measure ionic fluxes in microporous carbons for energy storage. *Nature Materials*, *8*(11), 872-875. https://doi.org/10.1038/nmat2559

Limousin, G., Gaudet, J. P., Charlet, L., Szenknect, S., Barthes, V., & Krimissa, M. (2007). Sorption isotherms: A review on physical bases, modeling and measurement. *Applied Geochemistry*, *22*(2), 249-275. https://doi.org/DOI:101016/japgeochem200609010

Liu, F., Liu, X., Ng, S.-C., & Chan, H. S.-O. (2006). Enantioselective molecular imprinting polymer coated QCM for the recognition of l-tryptophan. *Sensors and Actuators B: Chemical*, *113*(1), 234-240. https://doi.org/https://doi.org/10.1016/j.snb.2005.02.058

Lovander, M. D., Lyon, J. D., Parr, D. L., Wang, J., Parke, B., & Leddy, J. (2018). Critical Review—Electrochemical Properties of 13 Vitamins: A Critical Review and Assessment. *Journal of The Electrochemical Society*, *165*(2), G18-G49. https://doi.org/10.1149/2.1471714jes

Magar, H. S., Hassan, R. Y. A., & Mulchandani, A. (2021). Electrochemical Impedance Spectroscopy (EIS): Principles, Construction, and Biosensing Applications. *Sensors (Basel, Switzerland)*, *21*(19), 6578. https://doi.org/10.3390/s21196578

Matsumoto, K., Tiu, B. D. B., Kawamura, A., Advincula, R. C., & Miyata, T. (2016). QCM sensing of bisphenol A using molecularly imprinted hydrogel/conducting polymer matrix. *Polymer Journal*, *48*(4), 525-532. https://doi.org/10.1038/pj.2016.23

Menegazzo, N., Kranz, C., & Mizaikoff, B. (2012). Investigation of the anion uptake properties of cathodically electropolymerized poly(4-vinylpyridine) membranes [10.1039/C2NJ40156H]. *New Journal of Chemistry*, *36*(12), 2460-2466. https://doi.org/10.1039/C2NJ40156H

Meunier, C., Montérémal, J., Faure, P., & Ducros, V. (2015). Four years of LC-MS/MS method for quantification of 25-hydroxyvitamin D (D2+D3) for clinical practice. *J Chromatogr B Analyt Technol Biomed Life Sci*, *989*, 54-61. https://doi.org/10.1016/j.jchromb.2015.02.040

Mousavi, S. E., Amini, H., Heydarpour, P., Amini Chermahini, F., & Godderis, L. (2019). Air pollution, environmental chemicals, and smoking may trigger vitamin D deficiency: Evidence and potential mechanisms. *Environment International*, *122*, 67-90. https://doi.org/https://doi.org/10.1016/j.envint.2018.11.052

Munawar, H., Mankar, J. S., Sharma, M. D., Garcia-Cruz, A., Fernandes, L. A. L., Peacock, M., & Krupadam, R. J. (2020). Highly selective electrochemical

nanofilm sensor for detection of carcinogenic PAHs in environmental samples. *Talanta*, *219*, 121273. https://doi.org/https://doi.org/10.1016/j.talanta.2020.121273

Ngwanya, O. W., Ward, M., & Baker, P. G. L. (2021). Molecularly imprinted polypyrrole sensors for the detection of pyrene in aqueous solutions. *Electrocatalysis*, *12*(2), 165-175. https://doi.org/10.1007/s12678-020-00638-3

Núñez, L., Turiel, E., Martin-Esteban, A., & Tadeo, J. L. (2010). Molecularly imprinted polymer for the extraction of parabens from environmental solid samples prior to their determination by high performance liquid chromatography–ultraviolet detection. *Talanta*, *80*(5), 1782-1788. https://doi.org/https://doi.org/10.1016/j.talanta.2009.10.023

Ogawa, S., Kittaka, H., Nakata, A., Komatsu, K., Sugiura, T., Satoh, M., . . . Higashi, T. (2017). Enhancing analysis throughput, sensitivity and specificity in LC/ESI-MS/MS assay of plasma 25-hydroxyvitamin D(3) by derivatization with triplex 4-(4-dimethylaminophenyl)-1,2,4-triazoline-3,5-dione (DAPTAD) isotopologues. *J Pharm Biomed Anal*, *136*, 126-133. https://doi.org/10.1016/j.jpba.2016.11.030

Olcer, Y. A., Demirkurt, M., Demir, M. M., & Eroglu, A. E. (2017). Development of molecularly imprinted polymers (MIPs) as a solid phase extraction (SPE) sorbent for the determination of ibuprofen in water [Article]. *Rsc Advances*, *7*(50), 31441-31447. https://doi.org/10.1039/c7ra05254e

Petruzziello, F., Grand-Guillaume Perrenoud, A., Thorimbert, A., Fogwill, M., & Rezzi, S. (2017). Quantitative Profiling of Endogenous Fat-Soluble Vitamins and Carotenoids in Human Plasma Using an Improved UHPSFC-ESI-MS Interface. *Anal Chem*, *89*(14), 7615-7622. https://doi.org/10.1021/acs.analchem.7b01476

Rapuri, P. B., Gallagher, J. C., & Haynatzki, G. (2004). Effect of Vitamins D2 and D3 Supplement Use on Serum 25OHD Concentration in Elderly Women in Summer and Winter [journal article]. *Calcified Tissue International*, *74*(2), 150-156. https://doi.org/10.1007/s00223-003-0083-8

Rezayi, M., Ghayour-Mobarhan, M., Sany, S. B. T., Fani, M., Avan, A., Pasdar, Z., . . . Amiri, I. S. (2018). A comparison of analytical methods for measuring concentrations of 25-hydroxy vitamin D in biological samples [Review]. *Analytical Methods*, *10*(47), 5599-5612. https://doi.org/10.1039/c8ay02146e

Roth, D. E., Abrams, S. A., Aloia, J., Bergeron, G., Bourassa, M. W., Brown, K. H., . . . Whiting, S. J. (2018). Global prevalence and disease burden of vitamin D deficiency: a roadmap for action in low- and middle-income countries [Article]. *Annals of the New York Academy of Sciences*, *1430*(1), 44-79. https://doi.org/10.1111/nyas.13968

Sauerbrey, G. (1959). Verwendung von Schwingquarzen zur Wägung dünner Schichten und zur Mikrowägung. *Zeitschrift für Physik*, *155*(2), 206-222. https://doi.org/10.1007/BF01337937

Schneider, T. W., & Buttry, D. A. (1993). Electrochemical quartz crystal microbalance studies of adsorption and desorption of self-assembled monolayers of alkyl thiols on gold. *Journal of the American Chemical Society*, *115*(26), 12391-12397. https://doi.org/10.1021/ja00079a021

Song, Y., Lv, H., Hu, S., Yang, C., & Zhu, X. (2013). Electroactivity of Polyaniline in High pH Solutions. *Acta Chimica Sinica*, *71*, 999. https://doi.org/10.6023/A13020169

Streinz, C. C., Hartman, A. P., Motupally, S., & Weidner, J. W. (1995). The Effect of Current and Nickel Nitrate Concentration on the Deposition of Nickel Hydroxide Films. *Journal of The Electrochemical Society*, *142*, 1084-1089.

Sun, J., & Liu, Y. (2019). Unique Constant Phase Element Behavior of the Electrolyte-Graphene Interface. *Nanomaterials (Basel)*, *9*(7). https://doi.org/10.3390/nano9070923

Temova Rakuša, Ž., Pišlar, M., Kristl, A., & Roškar, R. (2021). Comprehensive Stability Study of Vitamin D3 in Aqueous Solutions and Liquid Commercial Products. *Pharmaceutics*, *13*(5), 617. https://doi.org/10.3390/pharmaceutics13050617

Viel, P., Palacin, S., Descours, F., Bureau, C., Derf, F., Lyskawa, J., & Salle, M. (2003). Electropolymerized poly-4-vinylpyridine for removal of copper from wastewater. *Applied Surface Science - APPL SURF SCI*, *212*, 792-796. https://doi.org/10.1016/S0169-4332(03)00105-3

Wang, Z., Li, H., Chen, J., Xue, Z., Wu, B., & Lu, X. (2011). Acetylsalicylic acid electrochemical sensor based on PATP–AuNPs modified molecularly imprinted polymer film. *Talanta*, *85*(3), 1672-1679. https://doi.org/https://doi.org/10.1016/j.talanta.2011.06.067

Wee Ling, J. L., Khan, A., Saad, B., & Ab Ghani, S. (2012). Electro polymerized 4-vinyl pyridine on 2B pencil graphite as ionophore for cadmium (II). *Talanta*, *88*, 477-483. https://doi.org/https://doi.org/10.1016/j.talanta.2011.11.018

Wei, X., Wang, G., Li, A., Quan, Y., Chen, J., & Wang, R. (2018). Application of Electrochemical Quartz Crystal Microbalance. *Progress in Chemistry*, *30*, 1701-1721. https://doi.org/10.7536/PC180132

Westbroek, P. (2005). 2 - Electrochemical methods. In P. Westbroek, G. Priniotakis, & P. Kiekens (Eds.), *Analytical Electrochemistry in Textiles* (pp. 37-69). Woodhead Publishing. https://doi.org/https://doi.org/10.1533/9781845690878.1.37

Wybranska, K., Szczubialka, K., & Nowakowska, M. (2008). Photochemical molecular imprinting of cholesterol [Article]. *Journal of Inclusion Phenomena and Macrocyclic Chemistry*, *61*(1-2), 147-151. https://doi.org/10.1007/s10847-007-9407-z

Yin, S., Yang, Y., Wu, L., Li, Y., & Sun, C. (2019). Recent advances in sample preparation and analysis methods for vitamin D and its analogues in different matrices. *TrAC Trends in Analytical Chemistry*, *110*, 204-220. https://doi.org/https://doi.org/10.1016/j.trac.2018.11.008

Zhai, D., Zhu, M., Chen, S., Yin, Y., Shang, X., Li, L., . . . Peng, J. (2020). Effect of Block Sequence in All-Conjugated Triblock Copoly(3-alkylthiophene)s on Control of the Crystallization and Field-Effect Mobility. *Macromolecules*, *53*(14), 5775-5786. https://doi.org/10.1021/acs.macromol.0c00598

Zotti, G., Schiavon, G., & Zecchin, S. (1995). Irreversible processes in the electrochemical reduction of polythiophenes. Chemical modifications of the polymer and charge-trapping phenomena. *Synthetic Metals*, *72*(3), 275-281. https://doi.org/https://doi.org/10.1016/0379-6779(95)03280-0

Zouaoui, F., Bourouina-Bacha, S., Bourouina, M., Abroa-Nemeir, I., Ben Halima, H., Gallardo-Gonzalez, J., . . . Errachid, A. (2020). Electrochemical impedance spectroscopy determination of glyphosate using a molecularly imprinted chitosan. *Sensors and Actuators B: Chemical*, *309*, 127753. https://doi.org/https://doi.org/10.1016/j.snb.2020.127753

VITA

PERSONAL INFORMATION

Surname, Name: Ölçer Altınsoy, Yekta Arya

EDUCATION

Degree	Institution	Year of Graduation
MSc	İzmir Institute of Technology	2016
BSc	İzmir Institute of Technology	2013

WORK EXPERIENCE

Year	Place	Enrollment
2019-presently	Kanat Paints and Coatings	R&D Researcher
2012	T. C. Ministry of Health Refik Saydam Hygiene Center Presidency	Trainee

PUBLICATIONS

- Olcer, Y. A., Demirkurt, M., Demir, M. M., & Eroglu, A. E. (2017). Development of molecularly imprinted polymers (MIPs) as a solid phase extraction (SPE) sorbent for the determination of ibuprofen in water [Article]. Rsc Advances, 7(50), 31441-31447. https://doi.org/10.1039/c7ra05254e.
- Demirkurt, M., Olcer, Y. A., Demir, M. M., & Eroglu, A. E. (2018). Electrospun polystyrene fibers knitted around imprinted acrylate microspheres as sorbent for paraben derivatives. Analytica Chimica Acta, 1014, 1-9. https://doi.org/https://doi.org/10.1016/j.aca.2018.02.016.
- Olcer, Y. A., Tascon, M., Eroglu, A. E., & Boyaci, E. (2019). Thin film microextraction: Towards faster and more sensitive microextraction [Review]. Trac-Trends in Analytical Chemistry, 113, 93-101. https://doi.org/10.1016/j.trac.2019.01.022.